Developing a powdR-based workflow for quantitative powder XRD analysis

---

MSc thesis N.M.A. Wichern

Master's Earth, Life and Climate

Utrecht University—department of Earth Sciences

September 2020 – May 2021

First supervisor: João P. Trabucho Alexandre

Second supervisor: Anita van Leeuwen-Tolboom

Table of Contents

Abstract

Powder XRD is a popular method for mineral quantification, but it often remains semi-quantitative due to difficulties such as preferred orientation in clays and feldspars. Preferred orientation effects are minimised when a full pattern summation quantification method is used. The quantitative powder XRD workflow developed here is centred around such a full pattern summation method: the R application powdR (Butler 2020). PowdR requires a reference library consisting of reference patterns of all to-quantify minerals. A reference library consisting of quartz, calcite, Ca-montmorillonite, labradorite, and microcline was developed here, and used to optimize the workflow. This optimized workflow consists of: 1) homogenising the samples in a McCrone mill; 2) scaling the reference patterns; 3) keeping the difference in intensity magnitude between reference patterns and sample pattern at a minimum; 4) using peak height and averaging multiple peak pairs to obtain the reference intensity ratio (RIR); 5) using manual instead of automatic full pattern summation, and an internal instead of an external standard, whenever possible; 6) using your own laboratory-specific reference library instead of an external one. The success of the peak-height approach is inconsistent with previous research—which has suggested a peak area-based RIR approach—and the cause of this success is unknown. When these recommendations are followed, quantification results with a relative bias of ≤10% can be obtained. When an external library is used instead, relative biases of ≥50% are reported. These large errors result in incorrect interpretations of paleoenvironment, paleoclimate, and diagenetic degree.

1. Introduction

Quantitative powder X-ray diffraction (XRD) is a widely used method to identify clay and non-clay minerals and to quantify individual minerals in mixtures (e.g. Raven and Self 2017 and references therein). Quantitative XRD of minerals in sedimentary rocks has been successfully applied to a range of research topics, including climate reconstruction (Scheffler, Buehmann, and Schwark 2006; Ortiz et al. 2009), diagenetic analysis (Boles and Franks 1979; Pearson and Small 1988; Środoń et al. 2006) and soil formation (Dere et al. 2013). Despite its popularity and advantages, this method still poses challenges. Some of these challenges are intrinsic to certain minerals, some arise from the mixing of different minerals. Consequently, powder XRD results often remain semi-quantitative rather than truly quantitative (e.g, Kuhlmann et al. 2004; Liu et al. 2008; Alizai et al. 2012; Egawa et al. 2015; Dinis et al. 2017).

Quantification requires relating the measured intensity of a mineral to its weight fraction in a mixture. To do this, various XRD methods have been developed in the past decades and improved upon, as summarised by e.g. Zhou et al. (2018). One of these methods is full pattern summation (Smith, Johnson, and Scheible 1987; Batchelder and Cressey 1998). Full pattern summation is based on the principle that an experimental pattern is composed of the individual patterns of all minerals that are present in the mixture.

Various software programmes have become available in the past decades to help with full pattern summation: FULLPAT (Chipera and Bish 2002), RockJock (Eberl 2003) and recently, powdR (Butler 2020). The latter is an R-based application. The R environment is user-friendly and comes with a wide range of data analysis and plotting possibilities. PowdR refines user-selected reference patterns of minerals until they fit the observed pattern using least-squares minimisation (Butler 2020). These reference patterns must be measured and uploaded into powdR's reference library before they can be used.

This reference library consists of intensity data and a reference intensity ratio (RIR) for each mineral. The RIR is a ratio between the intensities of the reference mineral to those of an internal standard, such as corundum (Chung 1974b; Hubbard and Snyder 1988). These intensity data are sensitive to sample preparation methods and instrument settings. Sample preparation determines the sample thickness, sample length, particle size, and degree of preferred orientation (e.g. Bish and Reynolds 1989). Instrument settings determine the size of diverging, receiving, and soller slits, the type of radiation, the goniometer radius, step-size, and counting time (e.g. Pecharsky and Zavalij 2009). All of these factors influence the final shape of the diffraction pattern. Thorough quantitative analysis thus requires that the intensities and RIRs be measured

on the same instrument that will be used for future analyses (Davis and Smith 1988; Davis, Smith, and Holomany 1989; Hillier 2000; Chipera and Bish 2013).

To set up this reference library in order to enable quantitative XRD at the Utrecht University XRD laboratory, several minerals commonly found in sedimentary rocks were chosen as a starting point: quartz, calcite, Ca-montmorillonite (smectite), labradorite (plagioclase feldspar), and microcline (K-feldspar). Quantitative XRD analysis of quartz and calcite is relatively uncomplicated. Quartz is a stable mineral that produces consistent XRD patterns; it can be used as an internal standard for this reason (Moore and Reynolds 1997). Calcite is also rather stable, but its peak positions and widths are subject to changes as a result of variations in magnesium content (Gavish and Friedman 1973 and references therein). The analysis of these two minerals becomes more complex when mixed with platy minerals such as clays. Unfortunately, the other minerals present an array of complications, both related to their structure and composition and to the analytical procedures required to measure them.

Clay minerals, in particular, present significant challenges—namely, (1) a lack of suitable reference minerals; (2) a preferred orientation; and (3) weak and broad peaks. Finding suitable reference minerals is challenging due to the large variation in chemical composition of clay minerals (Chipera and Bish 2013). This variation results from cation substitution in the tetra- and octahedral sheets and in the interlayer spaces, as well as mixed layering and varying degrees of disordered layering (Moore and Reynolds 1997; Środoń et al. 2001; Środoń 2006).

The platy habit of clay minerals gives them a preferred orientation, which complicates quantification. Quantitative XRD is based on the principle that intensities produced by diffraction on mineral-specific crystal lattice planes are proportional to the weight fraction of that diffracting mineral within the sample (Alexander and Klug 1948). This proportionality requires a random orientation of the particles in the powder, but the platy shapes resist randomisation. When present in a mixture with non-platy particles, such as quartz and calcite, the preferentially oriented platy particles diffract a disproportionate amount compared to spherical particles. This skews the intensities and thus the inferred weight fractions (e.g. Moore and Reynolds 1997). Minimising this preferred orientation requires special attention to sample preparation techniques (Bish and Reynolds 1989; Hillier 1999).

Finally, clay minerals have weak and broad peaks due to their small crystallite sizes (Moore and Reynolds 1997). To obtain stronger peaks, the intensity can be increased by increasing the beam width, but this results in a lower resolution, that is, broader peaks (e.g. Pecharsky and Zavalij 2009). For clay minerals, this

beam width induced peak broadening is not significant since their peaks are already intrinsically broad (Moore and Reynolds 1997). It does, however, affect other minerals when present in a mixture with clays minerals. In this case, some compromise between intensity and resolution is required.

Some of these complications intrinsic to clay minerals are also present in feldspar minerals. Feldspars exhibit a large range in composition due to the solid solution series between the Na-rich, K-rich and Ca-rich endmembers. They also have a preferred orientation due to their cleavage (Chipera and Bish 1995).

The full pattern summation method significantly reduces several of the complications outlined above. Preferred orientation errors are minimized when the whole pattern is used (Smith, Johnson, and Scheible 1987; Chipera and Bish 2013). In addition, disordered minerals with very weak and broad peaks are explicitly included in the analysis through its use of the whole pattern (Smith, Johnson, and Scheible 1987; Chipera and Bish 2013).

In this study, a powdR reference library—consisting of quartz, calcite, Ca-montmorillonite, labradorite, and microcline—has been developed and tested. With this library, quantitative results can be obtained from routine measurements. This enables preliminary quantitative XRD analysis at the Utrecht University sedimentological laboratory. This work may serve as a guide for further calibration of the method and expansion of the reference library.

2. Materials and methods

2.1. Materials

I procured powdered quartz from Merck (product code 107536) and powdered Ca-montmorillonite (95-100% pure, product code SAz-1) from the Clay Minerals Society. Whole rock samples of calcite, labradorite, and microcline were taken from the Utrecht University rock collection. Powdered corundum (α-Al_2O_3, ≥99.95% pure, product code 42573) from Alfa Aesar was used as an internal standard.

Table 1. Quartz grain size after grinding for 2, 6, and 10 minutes at 1500 rpm in the McCrone Mill.

Grinding time [min]	D50 [µm]	D90 [µm]
2 (4x30 s)	21.5	60.8
6	6.5	19.4
10	**4.5**	**14.5**

Table 2. Corundum grain size prior to grinding and after grinding for 10 seconds, 1 minute, and 2 minutes at 1500 rpm in the McCrone Mill.

Grinding time [min]	D50 [µm]	D90 [µm]
0	88.4	266.9
0.167	0.8	31.4
1	**0.5**	**11.2**
2	0.4	7.0

2.2. Sample preparation

The whole rock samples were crushed to <0.5 mm prior to wet grinding with isopropanol down to <10 μm in a Retsch McCrone Mill with zirconium oxide grinding elements. The powder samples did not require pre-treatment prior to grinding in the McCrone Mill. Grain size analysis of quartz on a Malvern Mastersizer 2000 indicated a grain size mode of 4.5 μm after 10 minutes of grinding at 1500 rpm (table 1). The internal standard corundum required grinding for 1 minute at 1500 rpm to decrease the size of the coarse fraction (table 2). All other samples have a hardness lower than that of quartz and are thus assumed to be equally fine or finer after grinding.

Mixtures were split in two sets that were homogenised manually and in the McCrone mill, respectively. This was done to test whether mechanical homogenisation in the McCrone mill—a more time-consuming process than homogenising by hand—produces better results and is thus worth the additional processing time. Manual homogenisation was done by tapping, shaking, and turning the container by hand for 5 minutes. Homogenisation in the McCrone mill was done by dry grinding for 1 minute at 1500 rpm.

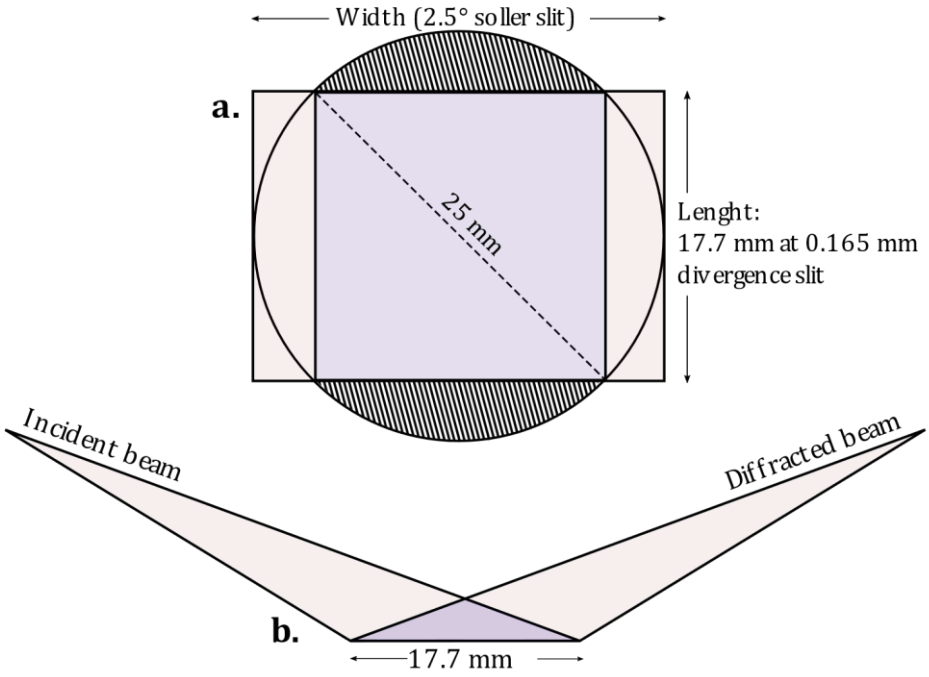

Figure 1. **a.** Schematic top-view of the geometry of the irradiated area of the diffractometer. The circle corresponds to the sample area, in which a 17.7 by 17.7 mm square fits. The purple rectangle corresponds to the total irradiated area, the width of which is defined by a fixed 2.5° soller slit, and the length by a variable divergence slit. There is some beam overspill onto the sample holder at the hatched areas. **b.** Side-view of the geometry of the irradiated area of the diffractometer, indicating the direction of the incidence of the beam.

2.3. Sample mounting

The powders were prepared as bulk samples by front-loading into a round PMMA sample holder with a diameter of 25 mm and a depth of 1 mm. To reduce preferred orientation, the sample holder was then covered with a glass plate, turned on its side, and tapped lightly. A maximum sample length of 17.7 mm was selected as a compromise between intensity loss and beam overspill (figure 1). For a goniometer radius of 28 cm and a minimum °2θ of 3°, this sample length corresponds to a divergence slit aperture of 0.165 mm (Moore and Reynolds 1997, equation 9.1). The sample depth required to attain infinite thickness of the sample was calculated using equation 2 in Bish and Reynolds (1989) (table 3). For a sample holder depth of 1 mm, all samples are infinitely thick. All samples were measured in duplicate after re-mounting.

Table 3. Mass absorption coefficients, linear absorption coefficients, calculated infinite thicknesses, and corresponding sample depths for each mineral for a °2θ range of 3° to 80°. The mass absorption coefficients were obtained from literature. The linear absorption coefficient is related to the mass absorption coefficient through $\boldsymbol{\mu} = \boldsymbol{\rho} * \boldsymbol{\mu}^*$, where ρ is the density of the material. [1]Bish and Reynolds (1989); [2]Moore and Reynolds (1997).

Mineral	Mass absorption coefficient μ*	Linear absorption coefficient μ	Infinite thickness [mg/cm2]	Required sample depth [mm]
Quartz	36.4	96.5[1]	17.6	0.07
Calcite	73.4[1]	194.5	8.8	0.03
Ca-montmorillonite	30[2]	66	25.9	0.12
Labradorite	50.6[1]	136.1	12.6	0.05
Microcline	50.6[1]	129.5	13.2	0.05

Table 4. Instrument settings for all experiments. A counting time of 0.85 s corresponds to >1000 counts above background for all dominant peaks. A step-size of 0.02 °2θ corresponds to 6-9 datapoints above the FWHM for the narrowest peak.

Instrument setting	**Value**
Voltage [kV]	40
Ampere [mA]	40
Radiation [Å]	1.5418 (CuKα)
Divergence slit [mm]	0.165
Primary soller slit [°]	2.5
Secondary soller slit [°]	not present
Measuring range [°2θ]	3-80
Step-size [°2θ]	0.02
Counting time [s]	0.85
Sample rotation [rpm]	15

2.5. Reference patterns

I first measured all samples and assessed their purity in Diffrac.EVA using the Powder Diffraction File (PDF) database from the International Centre for Diffraction Data (ICDD). To correct for potential peak shifts, I added 1 wt%

quartz to the Ca-montmorillonite, calcite, labradorite, and microcline samples. These samples were then homogenised in the McCrone mill and measured as bulk powders.

2.6. Data processing

All patterns were checked for peak shifts and stripped of the CuKα2 radiation component in Diffrac.Eva. A corundum crystal pattern was the peak position reference for samples containing corundum. For samples containing quartz, PDF 33-1161 (synthetic quartz) was used. Samples that contained neither were corrected by first correcting the quartz-spiked sample of that same mineral, and then using the corrected peak positions for the pure sample.

2.7. Reference Intensity Ratios

Full pattern summation in powdR uses reference intensity ratios (RIRs) to scale the intensity of a mineral pattern to that of an internal standard, which is corundum here (Butler 2020). To measure RIRs, 50:50 mixtures by weight of corundum with each mineral were made. These were homogenised manually and in the McCrone mill and measured as a bulk powder. From the measured patterns, RIRs were then calculated using the following equation:

$$RIR = \frac{Ia}{Ic} = \frac{Xc}{Xa} \times \frac{Ijc,rel}{Iia,rel} \times \frac{Iia}{Ijc} \quad (1)$$ (Schreiner 1995),

where a is the mineral of interest, c is the internal standard corundum, i and j are the mineral-corundum peak pairs, Ijc,rel is the intensity of corundum peak j in a pure corundum sample relative to the strongest corundum peak in a pure corundum sample—which is the 113 reflection—and Iia,rel is the intensity of mineral peak i in a pure mineral sample relative to the strongest mineral peak in a pure mineral sample. These strongest peaks were set to 100% (table 5). The standard deviation was estimated as follows:

$$s = \sqrt{\frac{\sum_{i=1}^{n}[\left(\frac{Ia}{Ic}\right)ij - RIRa,c]^2}{n-1}} \quad (2)$$

Mineral-corundum peak pairs were chosen based on their proximity to the mineral peaks (table 5). Peak overlap was avoided when possible, and peak regions were used when necessary (Chipera and Bish 1995). I initially applied the standard method of using the integrated peak area as a measure of intensity. When the RIRs calculated with this method resulted in the inaccurate quantification of quartz—the 'easiest' mineral in this study—I decided to calculate four different RIRs for each mineral, based on four different strategies:

1) the area of each peak was integrated to obtain its intensity I, and multiple peak pairs were used to obtain an average RIR. This will be referred to as the 'Area – multipeak' strategy.
2) The area of each peak was integrated to obtain its intensity I, and only the largest mineral peak and the corundum 113 peak were used to calculate a single RIR. This will be referred to as the 'Area – single peak' strategy.
3) The height of each peak was determined to obtain its intensity I, and multiple peak pairs were used to obtain an average RIR. This will be referred to as the 'Height – multipeak' strategy.
4) The height of each peak was determined to obtain its intensity I, and only the largest mineral peak and the corundum 113 peak were used to calculate a single RIR. This will be referred to as the 'Height – single peak' strategy.

As the corundum 113 peak overlaps almost completely with a calcite peak, the second-highest corundum peak, 35.14°2θ, was used here for the single peak strategies of calcite. This peak is almost as strong as the 113 peak—it has a relative height intensity of 96.6% and a relative area intensity of 88.4%.

The same routine was followed for the duplicate measurements and their results were incorporated into an average RIR for each mineral. This was done for both the McCrone mill homogenised and the manually homogenised mineral-corundum mixtures (table 6). The reference pattern (figure 2) and RIR of each mineral were loaded into powdR to establish the reference library (supplementary materials: reflib_patterns_NW.csv and reflib_RIRs_NW.csv).

Table 5. Mineral-corundum RIR peak pairs in °2θ. Single values indicate single peaks; a range of values indicates a peak region. Bolded peaks indicate the strongest peak used for the single peak RIR strategy.

	Corundum	**Quartz**	**Corundum**	**Calcite**
1	**43.33**	**26.64**	**35.13**	**29.41**
2	52.53	50.14	37.75	39.43
3	57.48	59.96	35.13	35.99
4	35.13	36.55	52.53	46.22-49.39

	Corundum	**Ca-montmorillonite**	**Corundum**	**Labradorite**
1	**43.33**	**5.84**	**43.33**	**27.21-28.60**
2	25.56	19.80	52.53	50.38-51.75
3	52.53	53.95	37.75	29.24-30.98
4	57.48	29.60	-	-

	Corundum	**Microcline**
1	**43.33**	**26.03-28.88**
2	57.48	48.71-51.43
3	52.53	29.04-31.48

RIRs should have a standard deviation that is <10% of the RIR value to be stable (Schreiner 1995). This has not been attained for all RIR strategies. Especially the minerals that exhibit preferred orientation—Ca-montmorillonite, labradorite, and microcline—show considerable relative errors. This is,

unfortunately, to be expected, and one of the reasons why RIRs should be averaged (Schreiner 1995). However, for most RIR strategies, the relative errors have been brought down to reasonable levels (Chipera and Bish 1995). Single peak strategies generally have a lower relative RIR error than multipeak strategies, indicating that the highest peaks are the most stable.

Table 6. Mineral RIRs relative to corundum, for McCrone mill and manually homogenised mineral-corundum mixtures, and for different RIR strategies. The first standard deviation is given next to the RIR value; the relative error of this standard deviation is given in brackets below the RIR value ($\boldsymbol{relative\ error} = \frac{\boldsymbol{standard\ deviation}}{\boldsymbol{RIR}} \times \mathbf{100}\%$).

	Quartz	Calcite	Ca-montmorillonite	Labradorite	Microcline
McCrone mill homogenised:					
Area – multipeak	4.49 ± 0.37 (8.2%)	3.33 ± 0.46 (13.8%)	5.15 ± 2.06 (40.0%)	2.08 ± 0.55 (26.4%)	2.71 ± 0.74 (27.3%)
Area – single peak	5.10 ± 0.03 (0.6%)	3.91 ± 0.01 (0.3%)	6.21 ± 0.61 (9.8%)	2.51 ± 0.48 (19.1%)	3.64 ± 0.30 (8.2%)
Height – multipeak	8.11 ± 0.81 (10.0%)	3.63 ± 0.59 (16.3%)	1.03 ± 0.29 (28.2%)	2.41 ± 1.07 (44.4%)	2.07 ± 0.89 (43.0%)
Height – single peak	9.20 ± 0.87 (9.5%)	4.55 ± 0.10 (2.2%)	1.32 ± 0.14 (10.6%)	3.19 ± 1.05 (32.9%)	3.18 ± 0.41 (12.9%)
Manually homogenised:					
Area – multipeak	5.40 ± 0.38 (7.0%)	4.26 ± 0.58 (13.6%)	3.59 ± 0.92 (25.6%)	2.89 ± 1.33 (46.0%)	3.83 ± 1.14 (29.8%)
Area – single peak	5.95 ± 0.01 (0.2%)	5.17 ± 0.24 (4.6%)	3.55 ± 0.33 (9.3%)	4.43 ± 0.62 (14.0%)	5.30 ± 0.16 (3.0%)
Height – multipeak	10.93 ± 0.83 (7.6%)	5.05 ± 0.96 (19.0%)	0.80 ± 0.19 (23.8%)	4.83 ± 3.11 (64.4%)	3.15 ± 1.52 (48.3%)
Height – single peak	12.20 ± 0.01 (0.1%)	6.58 ± 0.10 (1.5%)	0.78 ± 0.09 (11.5%)	7.65 ± 1.62 (21.2%)	5.12 ± 0.21 (4.1%)

2.8. Mixtures

To test the reference library, five synthetic rock mixtures were prepared and then homogenised (table 7; supplementary materials: synthetic_rock_mixtures_NW.xlsx). All synthetic rock mixtures, including those that contain Ca-montmorillonite, were prepared as a bulk powder to determine to what degree it is possible to accurately characterise and quantify a mixture in powdR without having to separate the clay fraction from the bulk sample.

Table 7. Mineral mixtures that mimic simplified sedimentary rocks. All mixtures contain 10 wt% corundum as an internal standard.

Mineral	Feldspathic quartz arenite wt%	Arkose wt%	Wacke wt%	Marl wt%	Shale wt%
Corundum	10.0	10.0	10.0	10.0	10.0
Quartz	78.3	48.3	41.3	5.3	13.7
Calcite	-	3.9	1.7	48.4	21.3
Ca-montmorillonite	5.8	-	27.2	36.3	55.0
Labradorite	3.8	22.9	8.5	-	-
Microcline	2.1	14.9	11.3	-	-

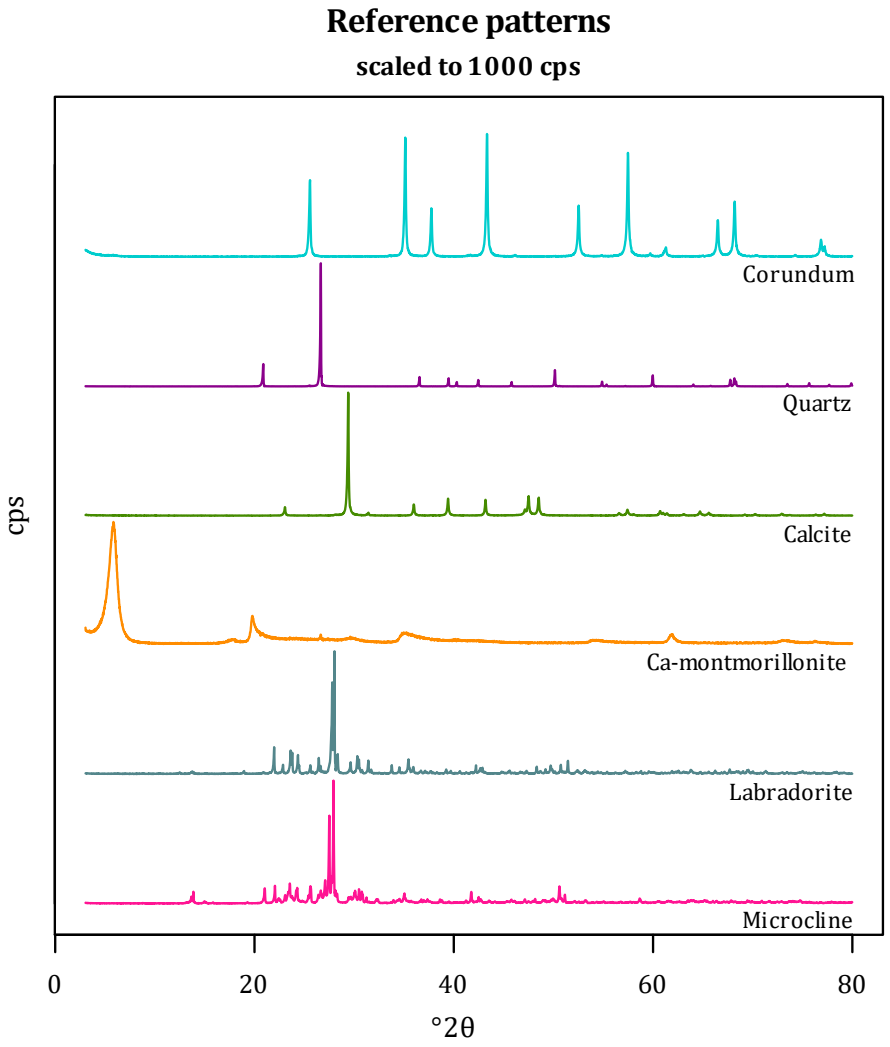

Figure 2. The reference patterns for all minerals used in this study, each scaled to a maximum of 1000 counts per second (cps).

2.9. powdR analysis

The R-application powdR, developed by Butler (2020), consists of three main components: (1) a reference library; (2) a manual full pattern summation

function ('fps') that requires the user to select already identified components of a mixture from the library; and (3) an automated full pattern summation function ('afps') that searches a specified library for fitting patterns and thus requires no previous identification. Both the fps and afps functions are based on least-squares minimisation to obtain an optimal fit between the reference and experimental patterns.

The user can choose to use an internal standard, which works through specifying the mineral ID and the concentration of the internal standard. If no concentration is specified, the external standard (adiabatic) method is used, in which all components are summed up to 100% (Chung 1974a). A detection limit can be set to constrain the number of minerals that may be identified with automated full pattern summation.

PowdR includes multiple solver functions ('BFGS', 'Nelder-Mead', and 'CG') and functions to be minimized ('Rwp', 'R', and 'Delta'). Testing by Butler and Hillier (2020) showed that the combination of 'BFGS' and 'Rwp' generally give the best results, and subsequently implemented these as the default settings. Here, preliminary testing found that the different functions result in minor differences in detected wt% and that the default combination gives good results. These settings have been used for all data presented here.

For this study, I used the synthetic rock mixtures to test the accuracy of manual full pattern summation in powdR. I applied both the internal and external standard methods and varied the detection limit. Since this study's reference library only contains 5 minerals plus the internal standard corundum, it is not suitable to test automatic full pattern summation. Therefore, a combined library has been made by adding this study's reference patterns to the in-built RockJock library (Eberl 2003; Butler 2020). The reference patterns in the RockJock library have been established with minerals of a different origin and have been measured on a different instrument. Carrying out automatic full pattern summation with this combined library thus tests two things: 1) the ability to identify the minerals in the sample without a priori knowledge, and 2) the ability to select this reference library's minerals over the same minerals in the RockJock library.

In addition to reference patterns, the RockJock database contains patterns of 8 synthetic mixtures that each consist of 6 minerals in varying weight percentages (including corundum as an internal standard). I used the RockJock library and these synthetic RockJock mixtures to assess the importance of establishing your own reference library in powdR. This was done by quantifying this study's mixtures with the RockJock library, and vice versa—all with manual instead of automatic full pattern summation to rule out any issues related to identification of the minerals.

A third use of the RockJock library and mixtures lies in the fact that applying the RockJock library to the RockJock mixtures gives accurate results (Butler and Hillier 2020, as well as testing done in this study). These RockJock quantification results can therefore serve as a standard regarding powdR's capabilities, to which this study's results can be compared.

PowdR results related to McCrone mill homogenisation were obtained by applying RIRs calculated from McCrone mill homogenised mineral-corundum mixtures to McCrone mill homogenised synthetic rock mixtures. The same applies to results related to manual homogenisation.

2.10. Method validation: Arén sandstone

So far, the reference library has been applied to this study's mixtures, which contain the exact same minerals that were used to create the reference library. In addition, the reference library has been applied to the RockJock mixtures. These do not only consist of different minerals, but are also measured on a different instrument and have thus two potential sources of error. To assess only the error related to differences in mineral origin, a natural rock sample was analysed in powdR. This rock sample is a fine-to-medium-grained calcarenite from the Upper Cretaceous upper Arén formation of the Tremp basin in Spain. It was collected along a road section near the village of Isona. Nagtegaal, Van Vliet, and Brouwer (1983) interpreted the upper Arén formation at this section as a delta/tidal inlet complex.

The Arén sample was ground in the McCrone mill to <10 µm and spiked with 10 wt% ground corundum. This mixture was then homogenised manually and in the McCrone mill. Note that, in contrast to the synthetic rock mixtures, the minerals present in this sample have been ground together rather than separately in the McCrone mill to reach the desired grain size. 'Manually' vs 'McCrone mill' homogenisation thus refers only to the adding and mixing of corundum here. After identification of the minerals using the PDF, the Arén sample was analysed in powdR to determine the degree to which the quartz and calcite reference patterns—and possibly other reference patterns as well—could be fitted to the quartz and calcite present in this sample (supplementary material: Arén_patterns_NW.csv).

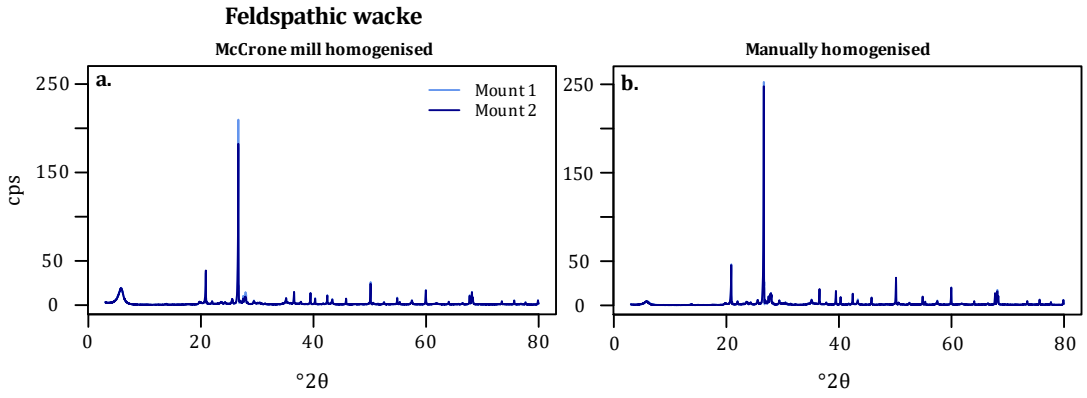

Figure 3. a. McCrone mill homogenised feldspathic wacke mixture, mounted and measured twice. **b.** Manually homogenised feldspathic wacke mixture, mounted and measured twice. For the second measurement ('mount 2'), the sample material was placed back into its container, shaken to mix it with the remaining sample material, and mounted again; all measurement settings were identical. The mounting reproducibility is good for both methods, but the intensities vary between the two

methods. McCrone mill homogenisation results in higher Ca- montmorillonite intensities and lower quartz intensities, while manual homogenisation has the opposite effect.

3. Results

3.1. Homogenisation effects

Reference intensity ratio (RIR) mixtures and synthetic rock mixtures mixed manually have higher mineral intensities than McCrone mill-homogenised mixtures (figure 3a-b). Consequently, RIR values calculated from manually homogenised mixtures are higher (table 6). An exception is Ca-montmorillonite, which has a higher intensity and RIR in McCrone mill homogenised mixtures (figure 3a-b; table 6). Mechanical homogenisation has been suggested to cause abrasion of the softer minerals by corundum, destroying some of their crystallinity (Schreiner 1995). There is, however, no amorphous material visible in the McCrone mill homogenised mixtures. The contrasting behaviour of clay and non-clay minerals suggests that non-clay particles physically obscure clay particles in manually homogenised mixtures—perhaps due to incomplete homogenisation—which increases their intensity relative to the clay minerals. RIRs calculated from manually homogenised mixtures work better when applied to manually homogenised samples and RIRs calculated from McCrone mill homogenised mixtures work better when applied to McCrone mill homogenised samples. McCrone mill homogenised mixtures results in a higher accuracy for each mineral (figures 4a-j, 5a-b).

3.2. RIR variations

Different minerals have different optimal RIR strategies—the optimal strategy being the one that results in the lowest bias during quantification (figure 4a-j, 5a-b; table 8)

Table 8. Optimal RIR strategy for each mineral.

Mineral	Optimal RIR strategy
Quartz	Height – single peak
Calcite	Area – single peak
Ca-montmorillonite	Height – single peak
Labradorite	Area – multipeak
Microcline	Height - multipeak

When the optimal RIR strategy for a mineral in a McCrone mill homogenised mixture is used, the mean of the corresponding dataset lies at or below a relative bias of 10% (figure 5a). This has been described as an 'excellent' result (Calvert, Palkowsky, and Pevear 1989, cited in Hillier 2000). However, as we need a standardized method to carry out quantitative powder XRD in our laboratory, a single RIR strategy must be decided on. To make this decision, I have looked at the relative biases of each strategy as this approach gives equal weight to minerals present in both high and low concentrations; the average absolute biases of each strategy can be found in appendix 1.1. For all the

minerals studied here, the height - multipeak strategy is the best compromise: for all minerals except Ca-montmorillonite, this strategy gives quantitative results (figure 4a, c, e, g, I; as defined by the $wt\%^{0.5}$ boundary of Hillier, 2000), and for quartz, calcite, and microcline, the results have a relative bias of 10 wt% on average (figure 5a).

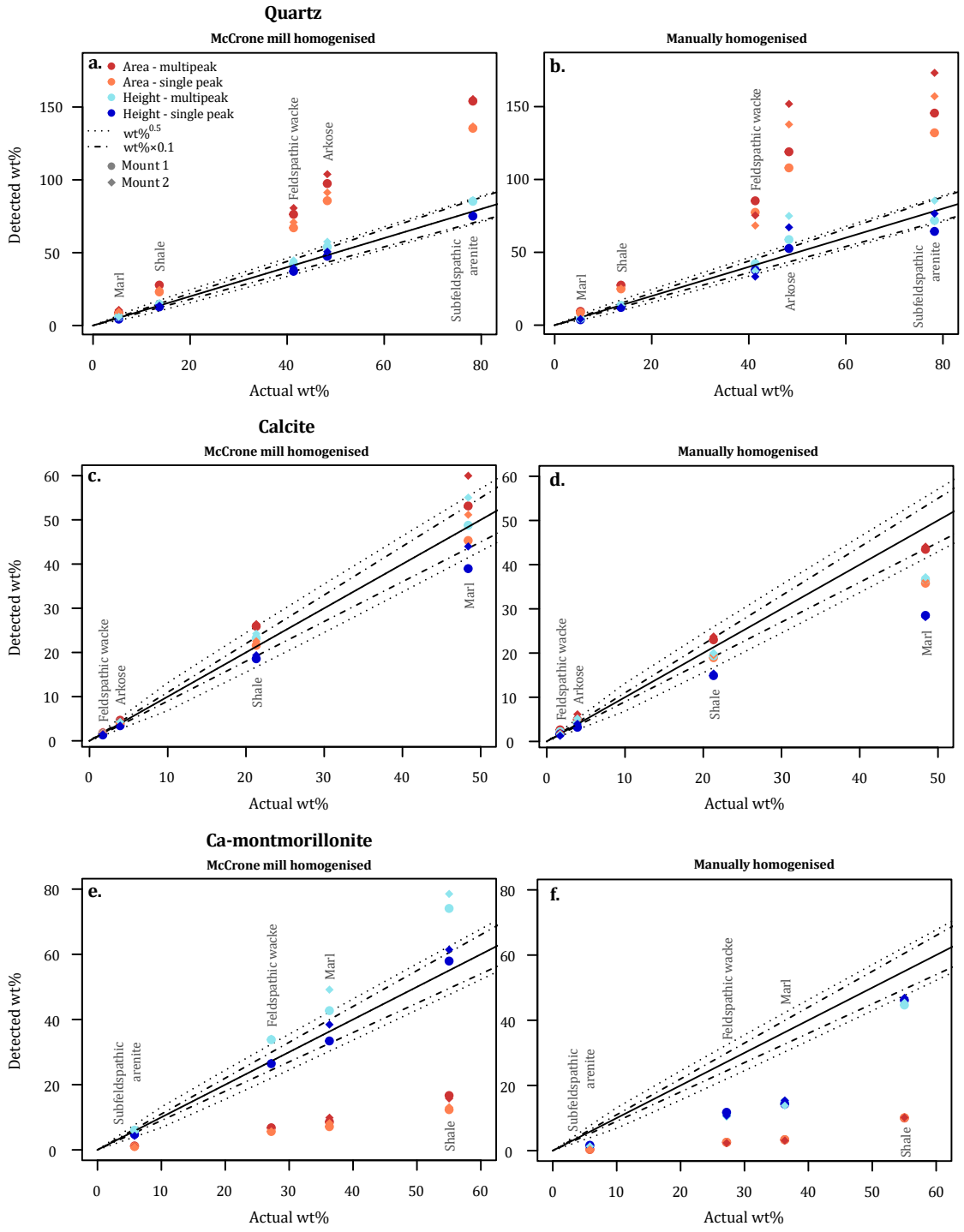

Figure 4. See next page for legend.

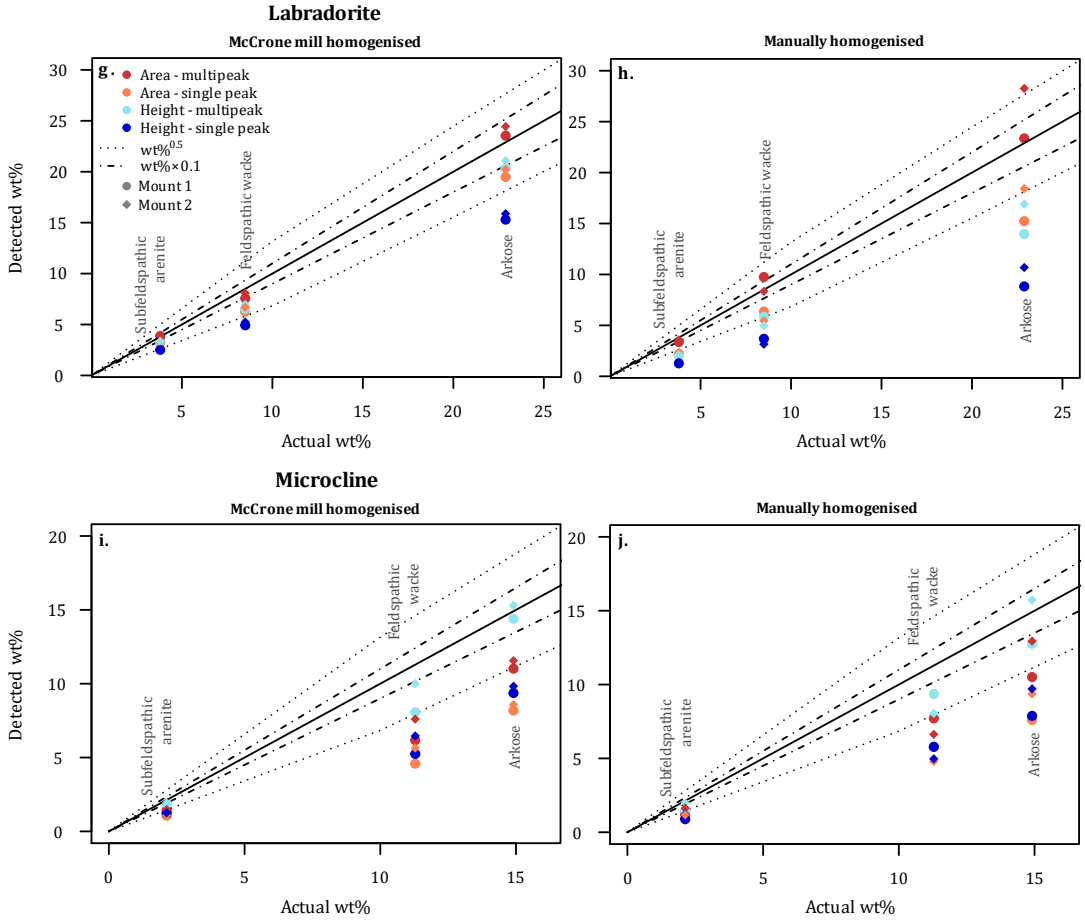

Figure 4. Scatter plots showing the actual vs detected wt% in the synthetic rock mixtures for each RIR strategy and for McCrone mill and manually homogenised mixtures, per mineral. Each mixture has been mounted and measured twice, and each dot represents a single measurement. Two margins around the 1:1 detected:actual solid black line represent the upper limits for quantitative measurement (wt%0.5, Hillier 2000) and 'excellent' results (wt%x0.1 or 10% relative bias, Calvert et al. 1989, cited in Raven and Self 2017). Different RIR strategies work best for different minerals, and McCrone mill homogenisation gives better results than manual homogenisation. When the optimal RIR strategy of each mineral in McCrone mill homogenised mixtures is considered, all measurements fall within the quantitative wt%0.5 limit, and almost all measurements fall within the excellent wt% x 0.1 limit. Apart from Ca-montmorillonite, the height-multipeak method gives quantitative results for each mineral.

3.3. Mounting reproducibility

There are minor differences between mounts of pure phases (figure 6) and mixtures (figure 3a-b), but the overall reproducibility is good: the difference in powdR quantification between two mounts of the same sample is on the order of a few wt% on average for each mineral when considering McCrone mill homogenised mixtures (figure 7). These few wt% differences can be caused by some inconsistencies with mounting such as surface irregularities (e.g., for quartz, which has no preferred orientation), preferred orientation (e.g., for Ca-

montmorillonite), and/or some inhomogeneities within the sample (e.g., for mixtures). Mounting reproducibility is similar for manually homogenised mixtures except for quartz, which has a much poorer reproducibility compared to quartz in McCrone mill homogenised mixtures (figure 7).

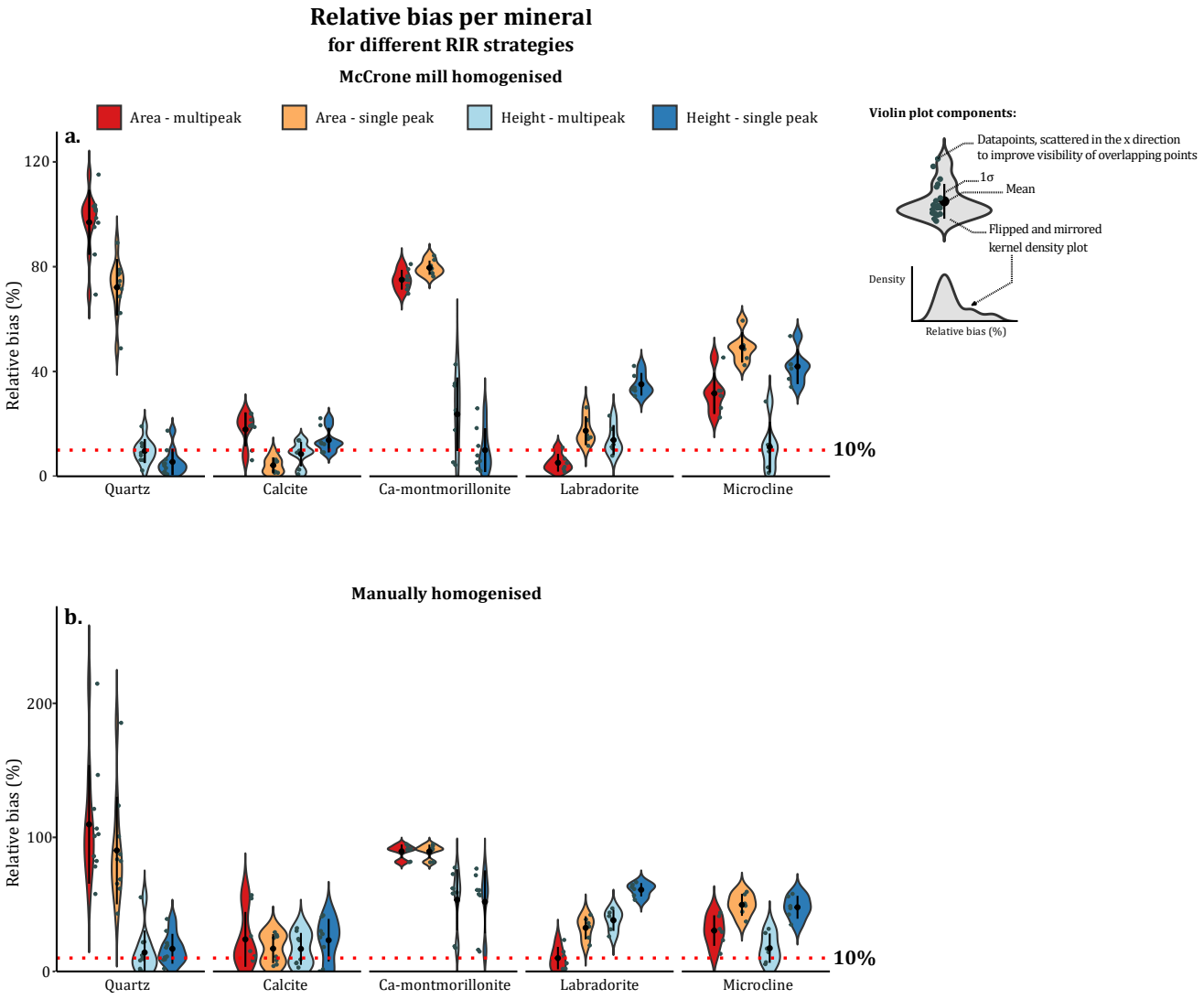

Figure 5. Violin plot showing the relative bias per mineral for each RIR strategy. **a.** results obtained from McCrone mill homogenised mixtures. **b.** results obtained from manually homogenised mixtures. Each violin contains data from all synthetic mixtures, each of which has been mounted and measured twice. Different minerals have different optimal RIR strategies. The RIR strategy trends are similar for McCrone and manually homogenised mixtures, but the results are better for McCrone mill homogenised mixtures. Only in the latter the optimal RIR strategy has a mean that is at or below 10% relative bias for almost all minerals (the exception being microcline, which has a slightly higher mean relative bias). Especially for Ca-montmorillonite, the results for manually homogenised mixtures are much poorer than for McCrone mill homogenised mixtures.

Mounting reproducibility is also similar across RIR strategies, with single peak strategies having a slightly better reproducibility (figure 8). This suggests that the highest peaks—on which the single peak RIRs are based—are the most stable. So, the height – multipeak RIR strategy—which I stated to be the best approach in the previous section—has a somewhat poorer reproducibility compared to single peak strategies. However, the benefit in terms of accuracy that you gain from using the height – multipeak RIRs is greater than the benefit in terms of reproducibility that you would gain from using the height – single peak RIR (figure 9), which is the best single peak strategy in terms of accuracy (figure 5a).

3.4. Scaled vs non-scaled reference patterns

Scaled reference patterns give better results than non-scaled reference patterns (figure 10a-b). After a reference pattern is scaled and fitted to the measured pattern, the RIR is used to calculate the wt%. Not scaling the patterns essentially results in a pattern's intensity being scaled relative to corundum twice: once in the fitting process, and then again through the use of the RIR. The maximum to which the reference patterns are scaled is arbitrary (Butler and Hillier 2020), as long as each reference pattern in the library is scaled to the same maximum cps or counts. The in-built RockJock reference library also consists of scaled reference patterns.

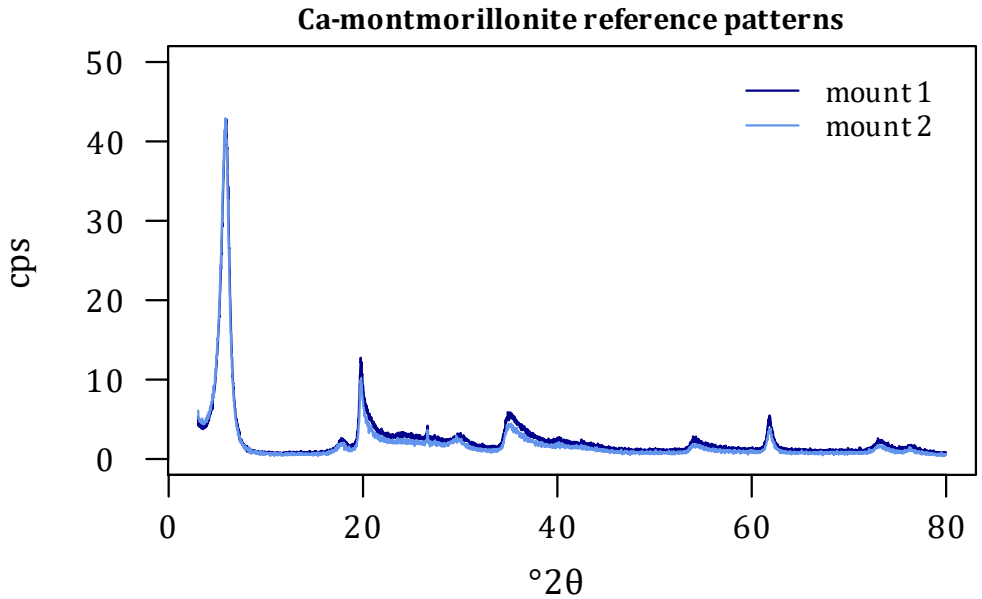

Figure 6. Two measurements of a pure Ca-montmorillonite sample. For the second measurement, the sample material was placed back into its container, shaken to mix it with the remaining sample material, and mounted again; all measurement settings were identical. The mounting reproducibility is good, even for a mineral with a strong preferred orientation such as Ca-montmorillonite.

3.5. Counts vs cps

As powdR works through pattern fitting, both cps and counts can be used as y-axis values for the samples and reference patterns. Both give accurate results, although some minor differences can arise. PowdR calculates the wt% of a mineral as follows:

$$wt\%_m = \frac{Coef_m}{Coef_{cor}} \times \frac{RIR_{cor}}{RIR_m} \times wt\%_{cor} \quad (3),$$

where 'm' is the mineral in question, 'cor' is the internal standard corundum, and 'Coef' is the scaling coefficient, which indicates how much the reference pattern in question has been scaled to fit the sample pattern (Butler 2020). The pattern itself, in counts or cps, only affects these coefficients in this equation.

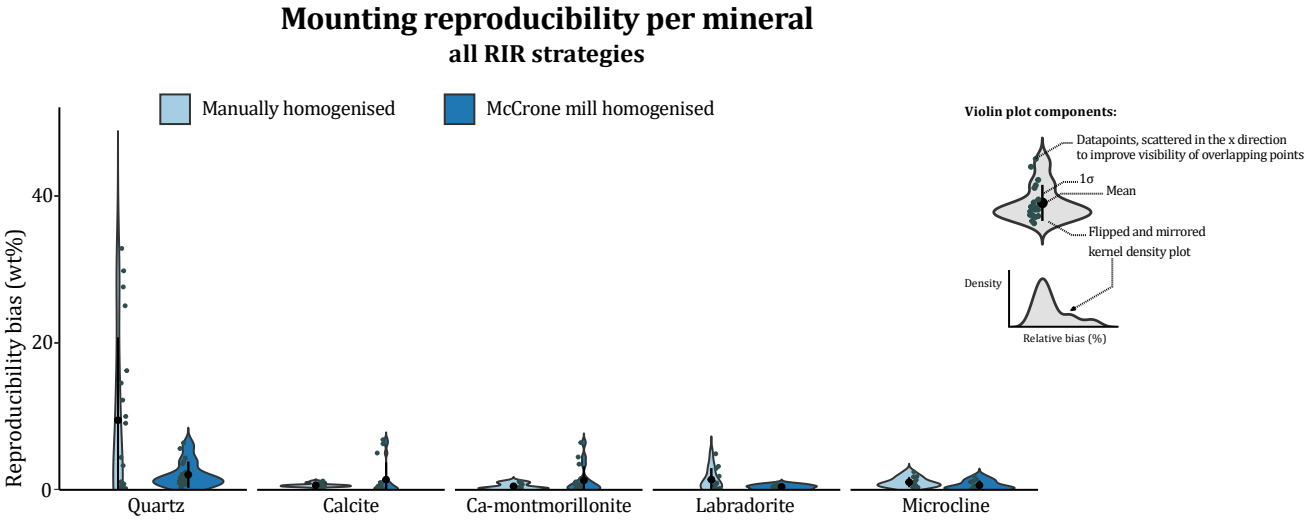

Figure 7. Violin plot showing mounting reproducibility biases—the difference in detected wt% between mount 1 and 2—per mineral and for McCrone mill and manually homogenised mixtures. Violin plot components are outlined on the right; a kernel density plot is a smoothened-out histogram. Each violin contains data from all synthetic mixtures and from all RIR strategies. Mounting reproducibility is similar for all minerals. It is also similar for both homogenisation methods, except for quartz, which has a much poorer reproducibility in manually homogenised mixtures.

When applying non-scaled reference patterns in cps to a non-scaled sample in cps, the result is the same as when applying non-scaled reference patterns in counts to a non-scaled sample in counts (table 9). However, when non-scaled reference patterns in cps are applied to a non-scaled sample in counts, the results are slightly different (table 10). This difference might arise from rounding the coefficients, which powdR does down to a limited number of decimals. Due to this limited number of decimals, the difference in magnitude of data in counts and data in cps becomes relevant. The magnitude of cps data is of the order of 100, while the magnitude of counts data is of the order of 10 000. Therefore, if you scale down a non-scaled reference pattern in counts

to a non-scaled sample pattern in cps, that scaled down reference pattern has a very low magnitude compared to the original reference pattern, resulting in a very small coefficient. With such a small coefficient, most of those decimals are occupied by zeroes (table 10). This effectively decreases the accuracy of the coefficient.

Table 9. Scaling coefficients calculated in powdR for quartz and corundum in the feldspathic wacke synthetic mixture, using counts and cps. When counts reference patterns are applied to counts samples and vice versa, the coefficient ratio is the same, and so will be the calculated wt%. Note that these reference patterns are not scaled, so plugging these coefficients into equation 3 will not result in the correct wt%.

Reference pattern		Sample		Scaling coefficients		
Unit	**Scaling**	**Unit**	**Scaling**	**$Coef_{cor}$**	**$Coef_{quartz}$**	**$Coef_{quartz}/Coef_{cor}$**
cps	not scaled	cps	not scaled	0.082254	0.375113	4.560435
counts	not scaled	counts	not scaled	0.082254	0.375113	4.560435

Table 10. Scaling coefficients calculated in powdR for quartz and corundum in the feldspathic wacke synthetic mixture, using counts and cps. When cps reference patterns are applied to counts samples and vice versa, the coefficient ratio is slightly different, and so will be the calculated wt%.

Reference pattern		Sample		Scaling coefficients		
Unit	**Scaling**	**Unit**	**Scaling**	**$Coef_{cor}$**	**$Coef_{quartz}$**	**$Coef_{quartz}/Coef_{cor}$**
cps	not scaled	counts	not scaled	13.45157	61.22386	4.551429
counts	not scaled	cps	not scaled	0.000504	0.002298	4.558679

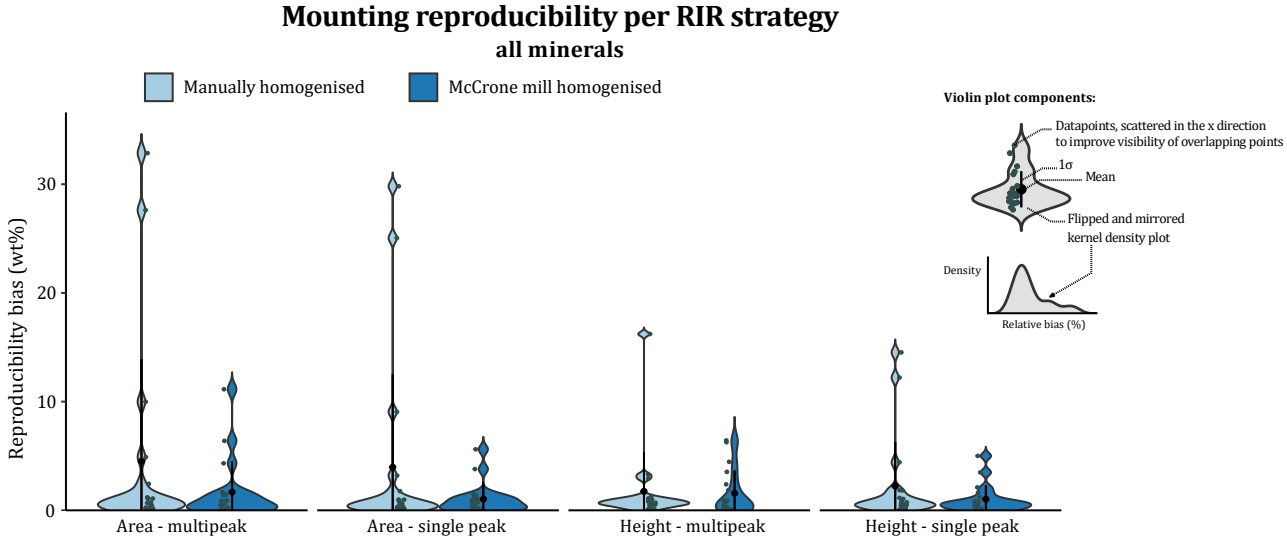

Figure 8. Violin plot showing mounting reproducibility biases—the difference in detected wt% between mount 1 and 2—per RIR strategy and for McCrone mill and manually homogenised mixtures. Each violin contains data from all synthetic mixtures and from all minerals. Mounting reproducibility is similar for all RIR strategies. McCrone mill homogenised mixtures have a better reproducibility for each RIR strategy, due to having less outliers with larger biases. These large biases in the manually homogenised mixture are all from quartz. Within the McCrone mill homogenised mixture results, single peak RIR strategies have a slightly better reproducibility.

Scaled reference patterns give better results than non-scaled reference patterns, as mentioned in the previous section. If you scale a reference pattern in cps and a reference pattern in counts to the same maximum, the difference between the two patterns disappears. The number that is scaled to is arbitrary, but to avoid mostly-zeroes-coefficients, the magnitude of the reference patterns should not be much larger than that of the sample pattern. The number that the reference patterns are scaled to, should reflect this.

In this study's library, all reference patterns have been arbitrarily scaled to 1000 cps and applied to non-scaled samples in cps. The sample patterns have not been scaled as full pattern summation quantification depends on the scaling of the reference patterns relative to one another, rather than the absolute scaling of the reference patterns relative to the sample pattern. Scaling the sample pattern as well, however, could be favourable when it has a very low intensity as it would mean downscaling the reference patterns significantly.

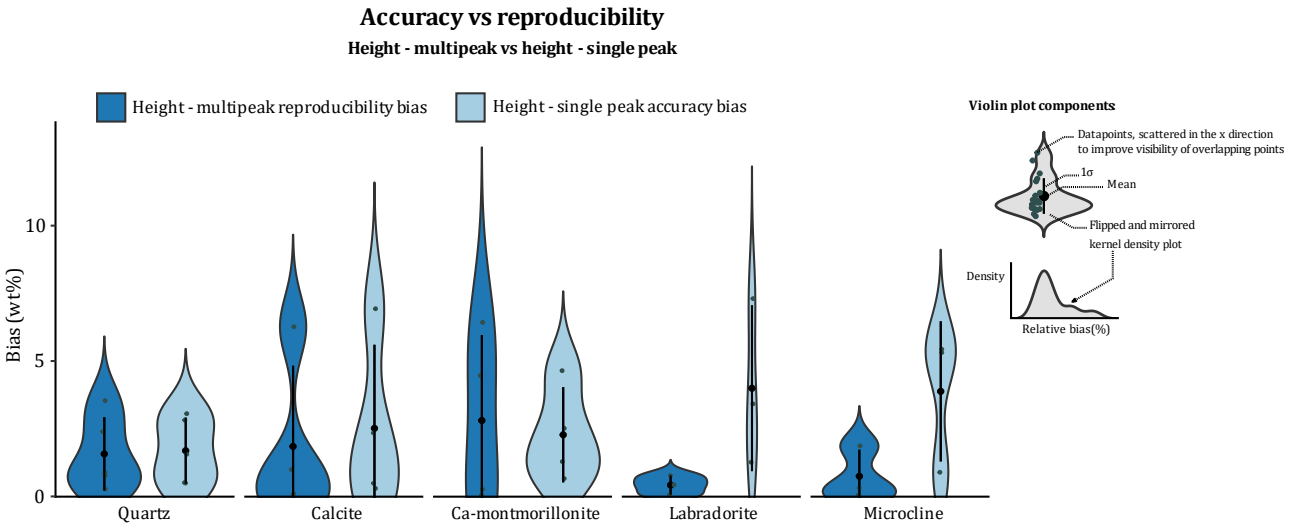

Figure 9. Violin plot comparing the reproducibility bias of the height-multipeak RIR strategy with the accuracy bias of the height-single peak RIR strategy, per mineral. 'Reproducibility bias' is defined as the difference between the detected wt% of mount 1 and mount 2. 'Accuracy bias' is defined as the difference between the actual wt% and the average of the detected wt% in mount 1 and mount 2. For all minerals except Ca-montmorillonite, the bias associated with the accuracy of the height - single peak method is larger than the bias associated with the reproducibility of the height - multipeak method. The slightly worse reproducibility of the height - multipeak method is thus no reason to discard this method in favour of the height - single peak method.

3.6. PowdR full pattern summation

3.6.1. This study's reference library

PowdR can accurately fit a calculated pattern to the measured patterns of the synthetic rock mixtures (figure 11a, b). A statistical measure of the goodness of fit between measured and fitted patterns is the weighted profile residual (Rwp), which is calculated by powdR and plotted in the right-hand corner of each

powdR fit plot. The lower the Rwp, the better the fit. Determining a threshold for accepted Rwp values is difficult due to various factors that can skew its value (Toby 2006). However, Rwp values for the McCrone mill homogenised synthetic rock mixtures quantified with this study's library (0.115-0.174, average 0.143, n=10) are similar, albeit a bit higher, than those for the RockJock mixtures that were accurately quantified with the RockJock library (0.114-0.142, average 0.127, n=8), and similar to accepted values from literature (e.g., Post and Bish, 1989). Visual assessment of the fits—which may tell you more than the Rwp value (Toby 2006)—indicates satisfactory results (figure 11b).

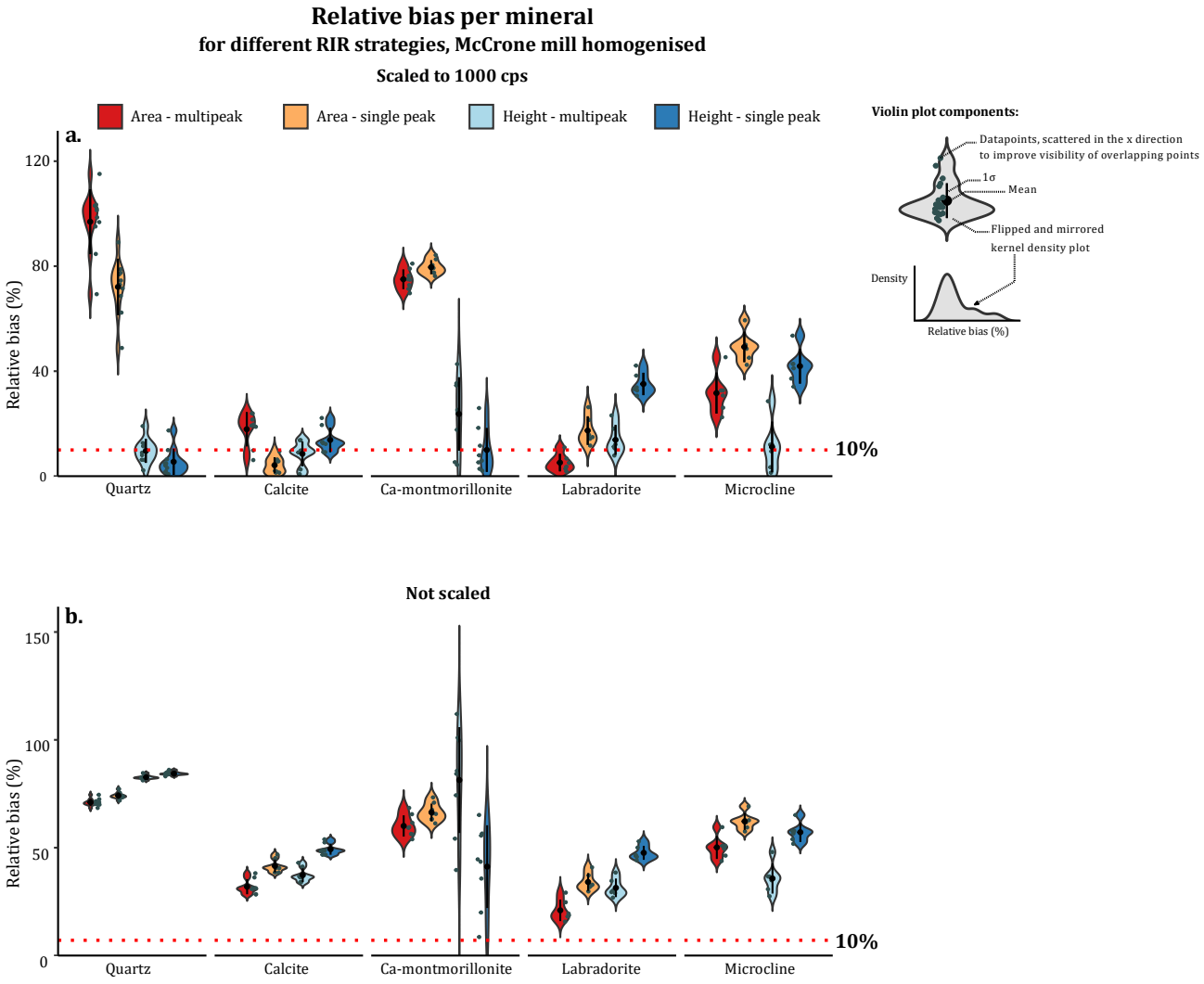

Figure 10. Violin plot showing the relative bias per mineral. **a.** relative biases obtained from using scaled reference patterns. **b.** relative biases obtained from using non-scaled reference patterns. Outcomes from powdR analysis with all RIR strategies were used, from McCrone mill homogenised mixtures only. Scaled reference patterns result in better results for each mineral.

The results of the external standard approach (e.g., summation of all detected components to 100 wt%; Chung 1974) vary. It increases the accuracy for some minerals but decreases it for others (figure 12).

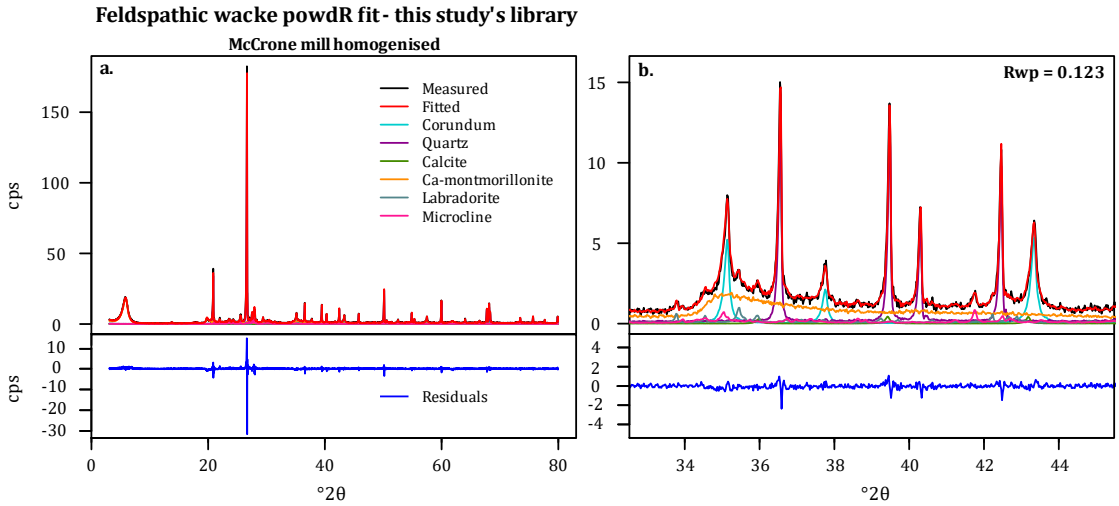

Figure 11. Manual full pattern summation powdR fit for the McCrone mill homogenised feldspathic wacke mixture, analysed with this study's reference library. **a.** the entire fitted pattern (top) and the residuals (bottom). **b.** a section of the pattern (top) and the residuals (bottom), highlighting the fit. The fit is good, indicated visually as well as by the Rwp value (panel b, top right).

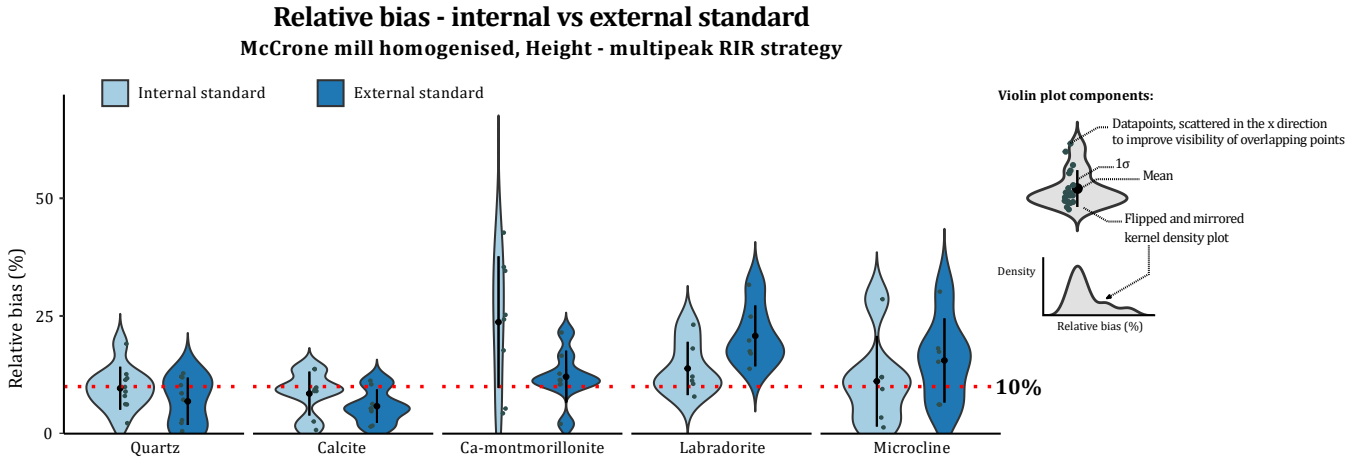

Figure 12. Violin plot showing the relative bias per mineral for using an external and an internal standard in McCrone mill homogenised mixtures. The height – multipeak RIR strategy has been used to obtain these powdR results. Using an external standard improves the accuracy for quartz, calcite, and Ca-montmorillonite, but decreases the accuracy for the two feldspar minerals.

3.6.2. Interlaboratory comparison: RockJock vs this study

The RockJock reference library (Eberl 2003) applied to the RockJock mixtures gives excellent results (appendix 2.1-2.4). Applied to one of this study's mixtures, the RockJock library gives a poor fit (figure 13a-b). Some of the weight percentages appear to be correct (table 11), but figure 13 indicates that this is an artifact of the severe underfitting of the measured pattern. Looking at each mineral in all five synthetic rock mixtures, using the RockJock library results in a similar relative bias for quartz and microcline compared to this study's

library, but a much higher relative bias for calcite, Ca-montmorillonite, and labradorite (figure 14). The RockJock library overestimated the amount of calcite by 30% on average. This corresponds to up to 13 wt%. The amount of labradorite was overestimated by 70% on average—almost twice the actual content, and up to 15 wt%. The 5.8 wt% of Ca-montmorillonite in the feldspathic arenite mixture was not detected by the RockJock library—even though it was explicitly specified to be present during manual full pattern summation—resulting in a relative bias of 100%. Fitting this study's reference library to a RockJock mixture also gives poor results (figure 15a-b; appendix 3.1). This is not merely a question of different RIRs, as switching out this study's height based RIRs for RockJock's RIRs gives similarly poor results (appendix 3.2).

Table 11. PowdR results for synthetic rock mixture feldspathic wacke (McCrone mill homogenised) quantified with the RockJock library. Settings: manual full pattern summation, 10 wt% corundum internal standard, no detection limit.

Mineral	Phase ID	RIR	Detected wt%	Actual wt%	Absolute bias [wt%]	Relative bias [%]
Corundum	CORUNDUM	1.00	10	10	0	0
Quartz	QUARTZ	3.54	41.99	41.32	0.67	1.63
Microcline	INTERMEDIATE_MICROCLINE	0.60	11.77	11.29	0.48	4.22
Labradorite	LABRADORITE	0.81	15.17	8.50	6.67	78.49
Calcite	CALCITE	2.15	2.54	1.70	0.84	49.44
Ca-montmorillonite	CA_MONTMORILLONITE	0.29	20.91	27.2	6.29	23.12
Total			**102.38**	**100**	**14.95**	

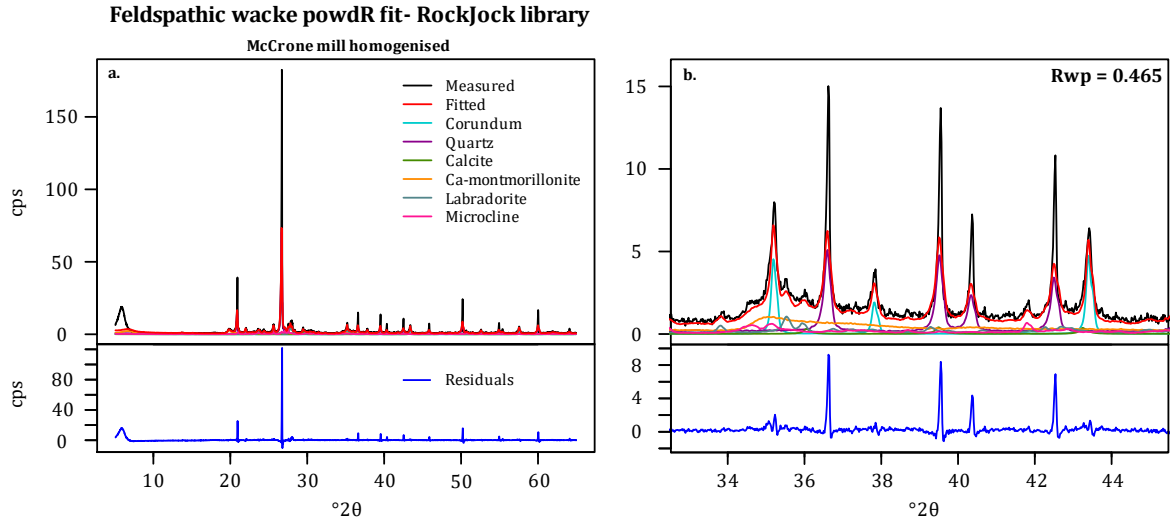

Figure 13. Manual full pattern summation powdR fit for the McCrone mill homogenised feldspathic wacke mixture, analysed with the RockJock reference library. **a.** the entire fitted pattern (top) and the residuals (bottom). **b.** a section of the pattern (top) and the residuals (bottom), highlighting the fit. The fit is poor, indicated visually as well as by the Rwp value (panel b, top right).

3.6.3. Automatic full pattern summation

When applying automatic full pattern summation and the combined library to this study's synthetic rock mixtures, powdR successfully selects this study's reference patterns instead of the RockJock library patterns of the same mineral (figure 16a-b; table 12). The feldspar patterns of this study's library and the RockJock library are similar, as the detected wt% of labradorite and microcline is spread over both libraries (table 12). When a detection limit is not applied, powdR also identifies many other minerals from the RockJock library in minor amounts. As a result, the detected wt% of the minerals that are present is less accurate than when using manual full pattern summation (table 12). This is not caused by the mismatch between the sample (from this study) and most of the reference patterns (from RockJock), as using automatic full pattern summation for quantification of a RockJock sample with the RockJock library also results in the misidentification of many minor mineral components (appendix 4.1). Using a detection limit of 1 wt% greatly reduces the number of incorrectly identified minerals, but this is at the risk of missing some minor components that are actually present. Calcite in the feldspathic wacke mixture was not identified when a 1 wt% limit was implemented (table 13), even though its actual wt% is 1.70 it has been detected at 1.24 wt% without a detection limit (table 12).

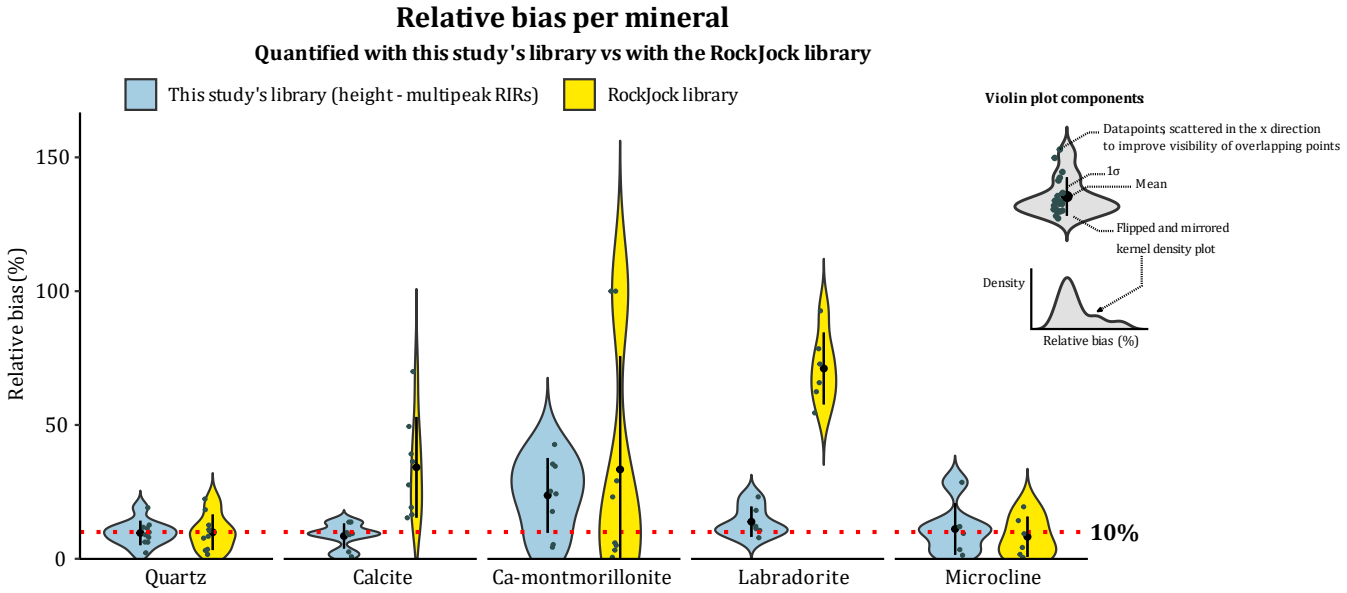

Figure 14. Violin plot comparing the relative bias per mineral present in this study's mixtures as quantified with this study's reference library (using the height - multipeak RIRs) and with the RockJock library. The results from this study's library are similar to, or better than the results obtained by the RockJock library, stressing the importance of setting up a laboratory-specific reference library. Note that the RockJock 100% relative bias obtained for Ca-montmorillonite is due to the RockJock library being unable to identify the small amount of Ca-montmorillonite in the feldspathic arenite mixture, even though it was specified as being present in powdR.

Table 12. Synthetic rock mixture Feldspathic wacke (McCrone mill homogenised) quantified with the combined library. Settings: automatic full pattern summation, 10 wt% corundum internal standard, no detection limit. Bolded minerals are from this study's library.

Mineral	Mineral ID	RIR	Detected wt%	Actual wt%	Absolute bias [wt%]
Corundum	**COR_AlfaAesar_1**	**1**	**10**	**10**	**0.00**
Quartz	**Q_Merck_1**	**8.11**	**39.69**	**41.32**	**1.63**
Calcite	**CAL_UU_1**	**3.63**	**1.24**	**1.7**	**0.46**
Ca-montmorillonite	**CA.MO_SAz1_1**	**1.03**	**33.25**	**27.2**	**6.05**
Labradorite	**LABRA_UU_1**	**2.41**	**4.60**	**8.5**	**3.90**
Microcline	**MICRO_UU_1**	**2.07**	**6.40**	**11.29**	**4.89**
Microcline	ORDERED_MICROCLINE	0.97	2.29	0	2.29
Sanidine	SANIDINE	0.72	1.07	0	1.07
Labradorite	LABRADORITE	0.81	5.56	0	5.56
Calcite	MG_CALCITE	1.06	0.39	0	0.39
Magnesite	MAGNESITE	1.23	0.23	0	0.23
Kaolinite	KAOLINITE_DRY_BRANCH	0.58	0.01	0	0.01
Mica	PHLOGOPITE_2M1	0.58	0.43	0	0.43
Sepiolite	SEPIOLITE	0.34	3.42	0	3.42
Anhydrite	ANHYDRITE	1.57	0.84	0	0.84
Olivine	FOSTERITE	0.54	1.09	0	1.09
Fluorite	FLUORITE	2.74	0.14	0	0.14
Opal	OPAL	0.34	2.18	0	2.18
Obsidian	OBSIDIAN	0.13	5.36	0	5.36
Ramsdellite	RAMSDELLITE	1.78	0.01	0	0.01
Sillimanite	SILLIMANITE	0.94	1.18	0	1.18
Gibbsite	GIBBSITE	0.98	0.39	0	0.39
Cinnabar	CINNABAR	4.94	0.20	0	0.20
Strontianite	STRONTIANITE	1.73	0.75	0	0.75
Celestine	CELESTINE	0.98	0.33	0	0.33
Sphalerite	SPHALERITE	5.08	0.13	0	0.13
Silver	SILVER	2.74	0.18	0	0.18
Diaspore	DIASPORE	1.17	0.78	0	0.78
Chalcopyrite	CHALCOPYRITE	2.89	0.86	0	0.86
Natrite	NATRITE	0.39	2.09	0	2.09
Nahcolite	NAHCOLITE	0.78	0.56	0	0.56
Total			**125.66**		**47.40**

Table 13. Synthetic rock mixture feldspathic wacke (McCrone mill homogenised) quantified with the combined library. Settings: automatic full pattern summation, 10 wt% corundum internal standard, 1 wt% limit. Bolded minerals are from this study's library.

Mineral	Mineral ID	RIR	Detected wt%	Actual wt%	Absolute bias [wt%]
Corundum	**COR_AlfaAesar_1**	**1**	**10**	**10**	**0**
Quartz	**Q_Merck_1**	**8.11**	**35.77**	**41.32**	**5.55**
Calcite	**CAL_UU_1**	**3.63**	**0**	**1.70**	**1.70**
Ca-montmorillonite	**CA.MO_SAz1_1**	**1.03**	**29.38**	**27.20**	**2.18**
Labradorite	**LABRA_UU_1**	**2.41**	**2.38**	**8.50**	**6.12**
Microcline	**MICRO_UU_1**	**2.07**	**4.38**	**11.29**	**6.91**
K-feldspar	ORDERED_MICROCLINE	0.97	4.48	0.00	4.48
Plagioclase	LABRADORITE	0.81	9.46	0.00	9.46
Sepiolite	SEPIOLITE	0.34	3.93	0.00	3.93
Obsidian	OBSIDIAN	0.13	15.66	0.00	15.66
Natrite	NATRITE	0.39	4.93	0.00	4.93
Total			**120.37**	**100**	**60.92**

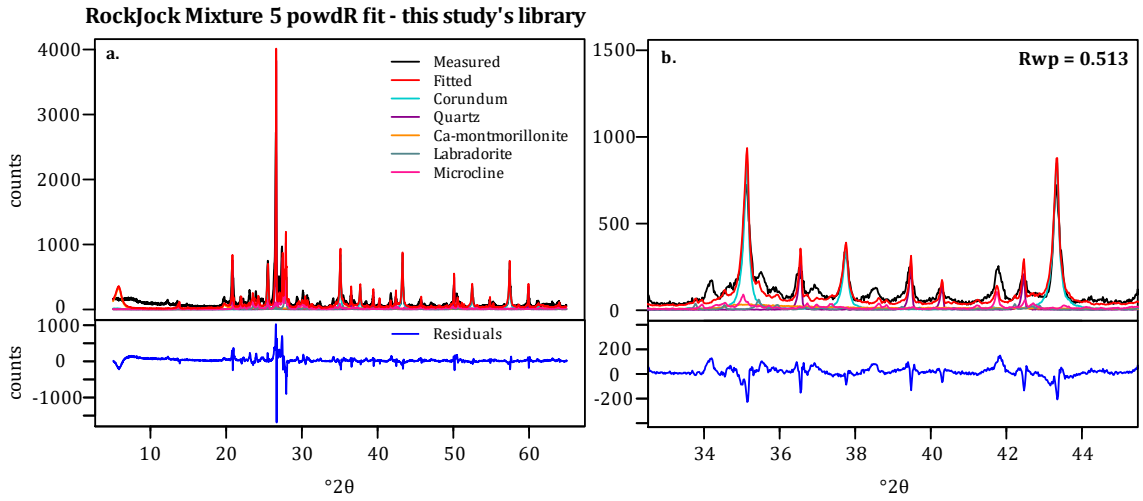

Figure 15. Manual full pattern summation powdR fit for RockJock mixture 5, analysed with this study's reference library. **a.** the entire fitted pattern (top) and the residuals (bottom). **b.** a section of the pattern (top) and the residuals (bottom), highlighting the fit. The fit is poor, indicated visually as well as by the Rwp value (panel b, top right). One component from mixture 5.4% kaolinite, is not present in this study's library, which accounts for part of the error.

3.6.4. Method validation: Isona Arén sandstone sample

Qualitative analysis with the PDF database indicated that this sample consists predominantly of quartz and calcite. I could not identify any other phases. Automatic full pattern summation in powdR with a 10 wt% corundum internal standard shows a decent fit between the measured and the fitted pattern when

the McCrone mill homogenised mixture was used (figure 17a-b). The goodness of fit—indicated by the Rwp—is not as good as for the synthetic mixtures, which to be expected as 1) the identified minerals are of a different origin, and 2) the sample may contain small amounts of unidentified minerals that are not present in this study's reference library. The fit for the manually homogenised mixture is very poor due to misalignment between the measured pattern and the reference patterns (figure 17d). The manually and McCrone mill homogenised Isona samples do not appear to be significantly misaligned relative to each other (appendix 5.1), so powdR's fitting algorithm may be exacerbating minor differences between the patterns. PowdR shifts the measured pattern relative to the reference patterns to optimize the fit up to a certain user-defined limit (default: 0.1° 2θ, value used here initially: 0.2° 2θ). Changing this limit does not solve the misalignment issue. Due to the poor fit of the manually homogenised mixture, only the results of the McCrone mill homogenised mixture will be discussed further.

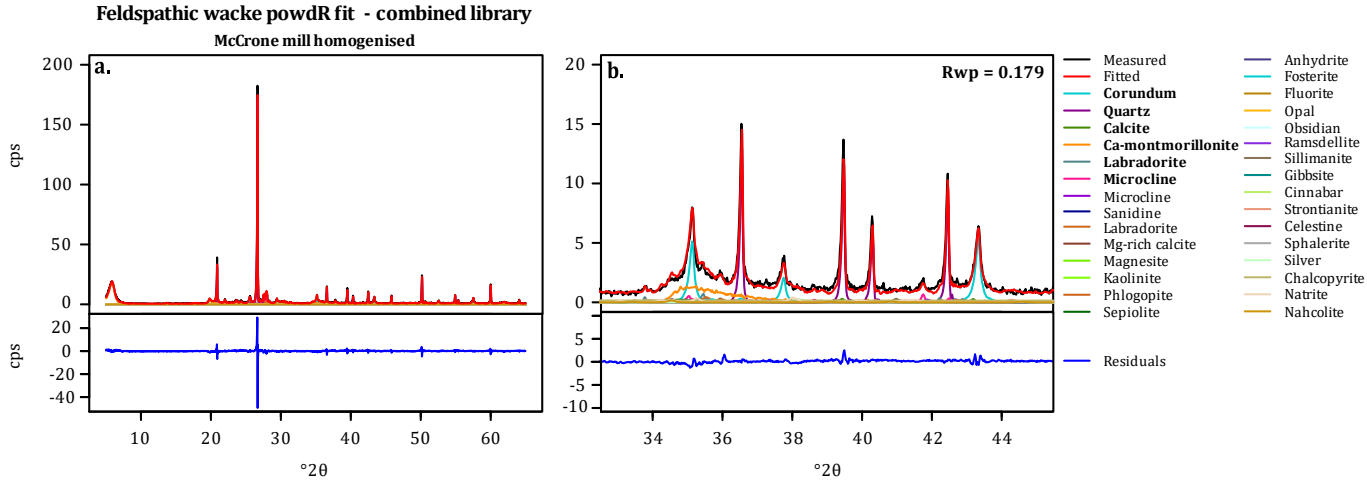

Figure 16. Automatic full pattern summation powdR fit for the McCrone mill homogenised feldspathic wacke mixture, analysed with the combined reference library. This library consists of this study's and RockJock's reference patterns. The reference patterns from this study have been scaled to 10000 to match the RockJock library. **a.** the entire fitted pattern (top) and the residuals (bottom). **b.** a section of the pattern (top) and the residuals (bottom), highlighting the fit. Bolded reference patterns are from this study's library. The fit is decent, indicated visually as well as by the Rwp value (panel b, top right), as most of the fit is obtained by fitting this study's reference patterns to the measured pattern. However, powdR also identified a large number of minerals from the RockJock library.

The McCrone mill homogenised Isona sample was quantified with different RIR strategies (figure 18a-f). According to powdR's quantification, it consists predominantly of quartz (43-90 wt%) and calcite (33-46 wt%), with minor amounts of microcline (approx. 1 wt%). Ca-montmorillonite and labradorite were also identified, but only at very low amounts (<0.6 wt% for Ca-montmorillonite and <0.06 wt% for labradorite).

The actual wt% of each mineral in this sample cannot be verified, but the total detected wt% can be used to assess the accuracy of each RIR strategy. The diffractogram indicates that the sample consists mainly of quartz and calcite,

two minerals that are present in this study's reference library. The total detected wt% is thus expected to be close to 100%. The total detected wt% is >78% for all RIR strategies (figure 18a). Both area-based strategies result in a total of >100% due to detecting 77-90 wt% quartz (figure 18b). The height-based strategies result in a total detected wt% of around 94% and 79% for multipeak and single-peak approaches, respectively (figure 18a).

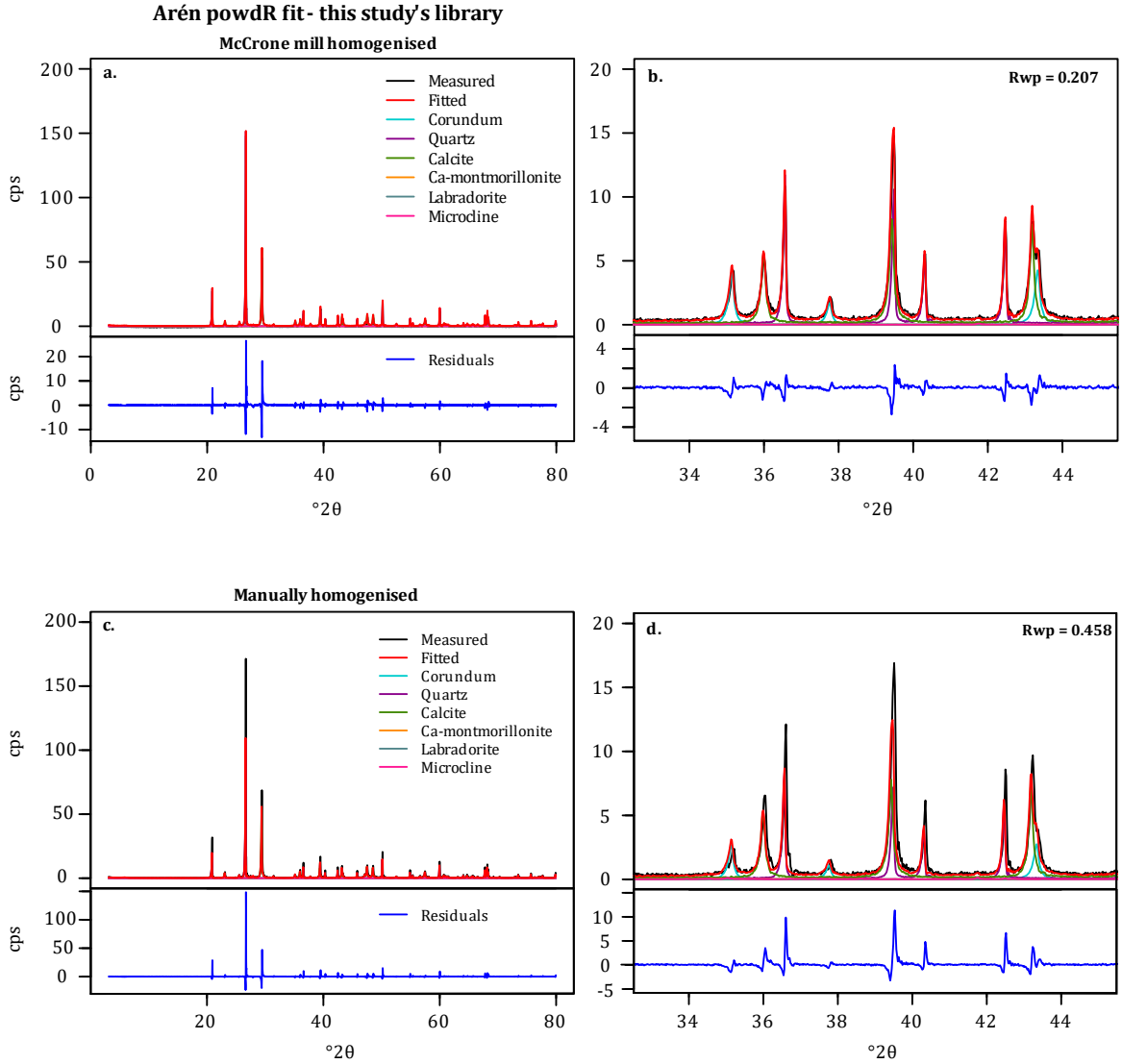

Figure 17. Automatic full pattern summation powdR fit for the McCrone mill and the manually homogenised Arén sample, analysed with this study's library. **a.** entire fitted pattern (top) and the residuals (bottom) of the McCrone mill homogenised sample. **b.** a section of this pattern (top) and the residuals (bottom), highlighting the fit. **c.** entire fitted pattern (top) and the residuals (bottom) of the manually homogenised sample. **d.** a section of this pattern (top) and the residuals (bottom), highlighting the fit. The fit for the McCrone mill homogenised sample is decent, indicated visually as well as by the Rwp value (panel b, top right). However, the fit for the manually homogenised sample is poor. All minerals present in this study's library have been identified by powdR in both samples.

4. Discussion

4.1. Arén Sandstone

4.1.1. Quantification

PowdR analysis indicated that the Arén sandstone sample consists predominantly of quartz and calcite. Minor amounts of Ca-montmorillonite and labradorite were also identified, but this may be an artifact of fitting to the background and/or minor differences between the reference minerals and the minerals in the sample. The height-multipeak RIR approach was most successful for quantification of the synthetic mixtures. When applied to the Isona sample, its total detected wt% is closest to 100%, suggesting that 'height-multipeak' is the best RIR strategy when applied to this unknown natural rock sample as well. I note that this sample consists mainly of quartz, for which the height-multipeak approach was shown to be almost as good as the optimal heigh-single peak approach, and calcite, which showed the least variation in detected wt% between the different RIR strategies. The results may have been different for a sample containing a large amount of labradorite, which was best quantified with an area based RIR strategy in the synthetic mixtures.

4.1.2. Paleoenvironmental implications

The Arén sandstone formation at the Isona section has been studied in detail by Nagtegaal, Van Vliet, and Brouwer (1983). They quantified its bulk composition through petrographic analysis and found more calcite than quartz: they obtained 33% quartz and feldspar and 66% carbonate (44% carbonate grains and 22% calcite cement) in the fine and medium-grained Arén sandstone and noted that the quartz content 'nowhere exceeds 50%' (p. 190). This is in line with this study's results of around 50% quartz and 45% calcite; the single sample analysed here, and the few thin sections analysed by Nagtegaal, Van Vliet, and Brouwer (1983), can represent more quartz-rich and more calcite-rich parts within the Arén sandstone. This study's results thus support the interpretation of the Arén sandstone at Isona as a mixed siliciclastic-carbonate high-energy shallow marine environment—likely an eb-tidal delta system based on stratal geometries—in which the quartz and feldspar were supplied from the hinterland and the carbonate was produced within the basin itself (Nagtegaal 1972; Nagtegaal, Van Vliet, and Brouwer 1983).

This interpretation was reached through analytical identification and quantification of the rock sample—either through thin-section analysis or quantitative powder XRD—which revealed a mixture of quartz and calcite, and very little K-feldspar. In the field, the rock is salmon-pink in colour, and fragments of K-feldspar can be seen with a hand-lens. In combination with the clearly visible quartz grains, this gives the rock a rather feldspathic arenite appearance. If not double-checked in the laboratory, this misidentification can result in a paleoenvironmental interpretation that is far too continental. The salmon-pink colour is suspected to be rhodolithic in origin, which is in line with the large amount of calcite in the sample. Rhodoliths are coralline algae that are purple-pink in colour (e.g., Foster et al. 2013), which have been reported in the

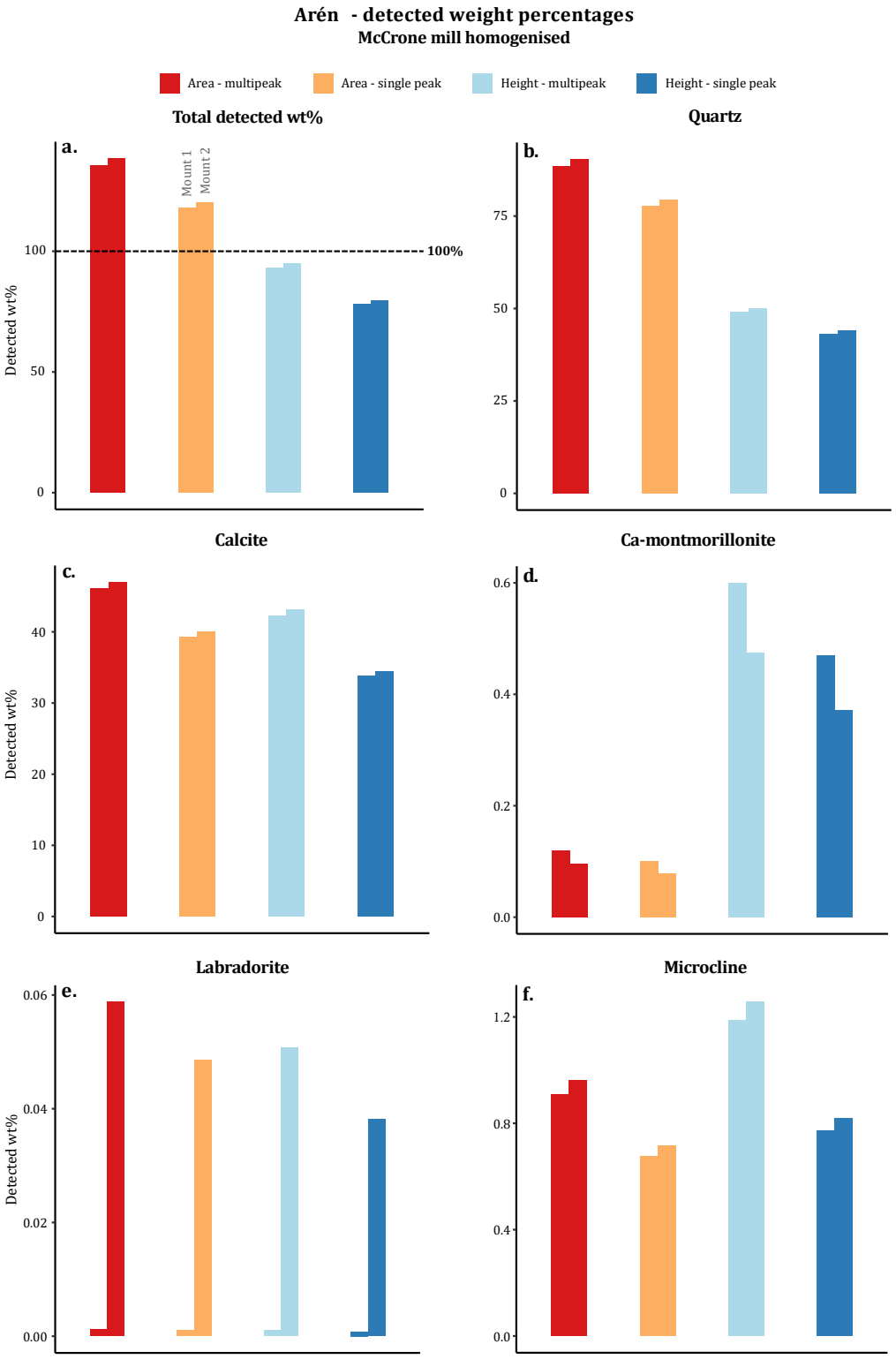

Figure 18. Bar plots showing the detected weight percentages for each RIR strategy in the McCrone mill homogenised Arén sample. **a.** total detected wt%. **b.** detected wt% quartz. **c.** detected wt% calcite. **d.** detected wt% Ca-montmorillonite. **e.** detected wt% labradorite. **f.** detected wt% microcline. Note the difference in scale for each mineral bar plot. The height – multipeak RIR strategy gives a total detected wt% that is closest to 100%. Ca-montmorillonite and labradorite are only detected in very minor amounts.

lower (e.g., Robles-Salcedo et al. 2013; Caus et al. 2016) and upper (Nagtegaal 1972; Nagtegaal, Van Vliet, and Brouwer 1983) Arén sandstone and fit the shallow-marine interpretation.

4.2. Reference intensity ratio (RIR) variations

Integrated peak intensity—here termed 'area-based RIR strategy'—is generally considered the best RIR strategy as it accounts for differences in peak width (e.g., Hubbard and Snyder 1988; Bish and Chipera 1994; Schreiner 1995; Chipera and Bish 1995; Hillier 2003). In this study, this is only the case for calcite and labradorite. I have not found an explanation for this phenomenon. The differences in optimal RIR strategy as applied in powdR might somehow be related to the peak widths of the various minerals relative to corundum and how that affects the iterative fitting process: Calcite, the mineral with a peak width most similar to corundum (figure 2), shows the least variability amount the different RIR strategies (figure 5a). Quartz and Ca-montmorillonite, which have peak widths that are either much narrower or broader than corundum, show the largest deviation between the area-based and height-based methods, and both are quantified best with heigh-based methods. The two feldspars are somewhere in between on both the peak-width spectrum and the spread in the results of each RIR strategy.

4.3. Accuracy assessment: comparison with RockJock and Reynold's Cup results

To assess the accuracy of this study's results within the framework of powdR, I compared the relative biases found in this study with those found in the RockJock dataset, as quantification with the RockJock dataset shows what powdR is capable of. To assess the accuracy of this study's results within a more general framework, I compared the relative biases found in this study with the outcomes of the Reynold's Cup round robin competition, as these results represent the current state of quantitative mineralogy.

Compared with the RockJock data (that is, the RockJock mixtures quantified with the RockJock library) this study's results have a somewhat poorer fit (average Rwp of 0.143 vs 0.127), a poorer absolute bias (average of 3.45 vs 1.06) and a poorer relative bias (compare figure 5a with appendix 2.2). There is thus still room for improvement within the powdR environment.

Comparison to the Reynold's Cup results is not as straightforward, as 1) in this study there was no issue of identification prior to (verifiable) quantification, which is one of the major sources of error in the Reynold's Cup (Raven and Self 2017); and 2) the synthetic mixtures presented here are much simpler than the ones used in the Reynold's Cup (Raven and Self 2017). Nevertheless, the Reynold's Cup results are a good way of assessing the state of quantitative mineralogy and where this study's results lie on the scale from poor to excellent quantification. When using relative biases, almost all measurements of this study fall within the $wt\%^{0.5}$ limits, and many of them fall within the 10% limits. When comparing this to the detected weight percentage spread in Raven and

Self (2017), this study's results are approximately average. By further optimizing the measurement routine at the Utrecht University XRD laboratory—for example, by implementing back-loading—we may be able to decrease the spread of the measurement results and decrease the relative biases down to ≤10% for all minerals.

4.4. Importance of developing a laboratory-specific reference library—and the consequences if you don't

The laboratory-specific reference library developed in this study enables quantitative powder XRD analysis of rock samples, down to a relative bias of ≤10% for some minerals. Conversely, using an external reference library—here, the RockJock library—can result in relative biases of >50% and even in leaving minor components completely unidentified. This can have far-reaching consequences.

The overestimation of the amount of calcite by the RockJock library can skew paleoenvironmental interpretations through overestimating the marine (or lacustrine) influence. It can also result in underestimating the degree of carbonate dissolution, which may lead to incorrect conclusions about lysocline position, ocean acidification, and CO_2 concentrations in the past, all of which are connected through the global carbon cycle (e.g., Ridgwell and Zeebe 2005 and references therein). Finally, it results in overestimation of the degree of diagenetic alteration when XRD is used to assess the preservation of aragonitic skeletons or shells (e.g., Marcano et al. 2015).

The severe overestimation of labradorite by the RockJock library will make a sandstone appear to be much more feldspathic than it actually is. This suggests a much less mature rock, as feldspar is more labile than quartz (e.g., Nesbitt and Young 1989 and references therein). Plagioclase is especially labile, more so than K-feldspar (Nesbitt and Young 1989; Nesbitt, Fedo, and Young 1997, and references therein), so overestimating the amount of labradorite relative to K-feldspar will make a rock seem very immature. Misjudging the maturity can affect further interpretations—a different provenance, a different weathering regime, and, in turn, a different tectonic setting or a different climate regime (e.g., Suttner and Dutta 1986; Nesbitt and Young 1996; Nesbitt, Fedo, and Young 1997).

Entirely missing 5.8 wt% of clay can result in overestimating the transport energy of the depositional environment, as clay particles require quiet water to be deposited (Hjulström 1939; Sundborg 1956). In addition, errors in smectite quantification will hamper diagenetic illite-smectite analysis: Smectite is converted to illite with increasing temperature and thus burial depth (Boles and Franks 1979; Pearson and Small 1988; Środoń et al. 2006). Within certain constraints, the percentage of smectite can be used as a palaeothermometer (Środoń et al. 2006), although it must be noted that smectite quantification for this purpose may require oriented clay measurements instead of the bulk measurements (Środoń et al. 2006).

This study has shown the importance of measuring laboratory-specific reference patterns and calculating RIRs for quantitative analysis in powdR, something that has already been stressed by many authors when it comes to quantitative powder XRD analysis (e.g., Smith, Johnson, and Scheible 1987; Hillier 2000; 2003; Chipera and Bish 2013). Future work in this area should therefore focus on extending this study's reference library to ultimately include all minerals commonly found in sedimentary rocks.

5. Recommendations

In view of the data presented in this study, the following recommendations are given for carrying out quantitative XRD analysis with powdR in the Utrecht University XRD laboratory:

Sample homogenisation: homogenise RIR mixtures and spiked samples in the McCrone mill, rather than manually, as this improves the quantification accuracy.

Scaling: scaling all reference patterns to the same arbitrary number of counts or cps improves the accuracy. In this study, all reference patterns have been scaled to 1000 cps. Scaling the sample patterns is not required, but it is not detrimental either; it is a question of preference. It may be useful in cases with a very low (<100 cps) intensity.

Counts vs cps: either counts or cps can be used, and they can be used together, as long as 1) the reference patterns are scaled and 2) the intensity of the reference patterns is not several magnitudes larger than that of the sample pattern. For consistency, it is suggested to choose one and stick to it.

RIR strategy: the height-multipeak RIR strategy is the best compromise for the minerals presented in this study. It is recommended to follow this strategy for new minerals. However, the accuracy of this strategy should be tested occasionally for new mineral additions to the library—especially for minerals that are of a completely different structural nature than the minerals presented here. When determining RIRs for new reference minerals, the area-based RIRs should be calculated as well and stored, so that they can be easily retrieved and applied when new insights favouring an area-based approach emerge.

Automatic pattern summation and external standards: using automatic pattern summation results in the identification of a large number of minerals in minor amounts. A detection limit can be set to limit the number of detected minerals, but this can result in missing some trace minerals. Identification of the components in a sample prior to quantification is the recommended strategy. In addition, it is important to assess the probability of certain minerals being present in a rock sample: if powdR identifies platinum in a calcarenite, some alarm bells should start ringing. This was also noted by Raven and Self (2017). Identification is also important for powdR analysis without an internal standard. As you can no longer assess the quality of the quantification or indirectly identify missing components when using an external standard, it is only recommended to forgo using an internal standard when you are confident that all components present are identified correctly.

Reference library: the current reference library consists of five minerals plus corundum as an internal standard. While being a good starting point, this is of course very limiting; in contrast, the RockJock library in powdR contains 169 minerals. New minerals should be added to the reference library, following the recommendations outlined above. On one hand, this expansion should focus on obtaining a wide range of minerals—like adding kaolinite, pyroxene, or pyrite to the current library. On the other hand, it should focus on obtaining many different varieties of certain minerals—like adding high-Mg calcite, different kinds of montmorillonite, or even different Ca-montmorillonites from different sources—in order to combat the issue of a lack of suitable reference minerals.

6. Conclusions

A reference library for the full pattern summation R application powdR has been developed, consisting of 5 minerals commonly found in sedimentary rocks: quartz, calcite, Ca-montmorillonite, labradorite, and microcline. With this reference library, quantitative—rather than semi-quantitative—X-ray diffraction (XRD) analysis is possible with routine bulk measurements. For quartz, calcite, and microcline, the average relative bias is down to ≤10%, which has been regarded as an excellent result (Calvert, Palkowsky, and Pevear 1989, cited in Hillier 2000). In order to set up this reference library, a quantitative XRD analysis workflow was developed from sample preparation to data analysis in powdR. This has resulted in the development of several recommendations for successful analysis. This study's results emphasize the importance of using laboratory-specific reference patterns and RIRs for quantitative powder XRD analysis. Using an external reference library instead of your own laboratory-specific library can result in relative biases of ≥50% and absolute biases as large as 15 wt%. Biases of this order can lead to errors in paleoenvironmental interpretations, paleoclimatic studies, and diagenetic estimates.

7. References

Alexander, Leroy, and Harold P. Klug. 1948. 'Basic Aspects of X-Ray Absorption in Quantitative Diffraction Analysis of Powder Mixtures.' *Analytical Chemistry* 20 (10): 886–89. https://doi.org/10.1021/ac60022a002.

Alizai, Anwar, Stephen Hillier, Peter D. Clift, Liviu Giosan, Andrew Hurst, Sam VanLaningham, and Mark Macklin. 2012. 'Clay Mineral Variations in Holocene Terrestrial Sediments from the Indus Basin.' *Quaternary Research* 77 (3): 368–81. https://doi.org/10.1016/j.yqres.2012.01.008.

Batchelder, Meryl, and Gordon Cressey. 1998. 'Rapid, Accurate Phase Quantification of Clay-Bearing Samples Using a Position-Sensitive X-Ray Detector'. *Clays and Clay Minerals* 46 (2): 183–94. https://doi.org/10.1346/CCMN.1998.0460209.

Bish, David L., and Steve J. Chipera. 1994. 'Accuracy in Quantitative X-Ray Powder Diffraction Analyses'. *Advances in X-Ray Analysis* 38: 47–57. https://doi.org/10.1154/S0376030800017638.

Bish, David L., and Robert C. Reynolds. 1989. 'Sample Preparation for X-Ray Diffraction'. In *Modern Powder Diffraction*, 20:73–100. Reviews in

Mineralogy & Geochemistry. Washington, D.C.: Mineralogical Society of America. https://doi.org/10.1515/9781501509018-007.
Boles, James R., and Stephen G. Franks. 1979. 'Clay Diagenesis in Wilcox Sandstones of Southwest Texas: Implications of Smectite Diagenesis on Sandstone Cementation'. *Journal of Sedimentary Petrology* 49 (1): 55–70.
Butler, Benjamin. 2020. 'PowdR: Full Pattern Summation of X-Ray Powder Diffraction Data'. https://cran.r-project.org/web/packages/powdR/vignettes/powdR_vignette.html.
Butler, Benjamin, and Stephen Hillier. 2020. 'PowdR: An R Package for Quantitative Mineralogy Using Full Pattern Summation of X-Ray Powder Diffraction Data'. *Preprint Submitted to Computers and Geosciences*, 33. https://doi.org/10.1016/j.cageo.2020.104662.
Calvert, C.S., D.A. Palkowsky, and D.R. Pevear. 1989. 'Combined X-Ray Powder Diffraction and Chemical Method for the Quantitative Mineral Analysis of Geologic Samples.' *Clay Mineral Society Workshop Lecture* 154.
Caus, Esmeralda, Gianluca Frijia, Mariano Parente, and Raquel Robles-Salcedo. 2016. 'Constraining the Age of the Last Marine Sediments in the Late Cretaceous of Central South Pyrenees (NE Spain): Insights from Larger Benthic Foraminifera and Strontium Isotope Stratigraphy.' *Cretaceous Research* 57: 402–13. http://dx.doi.org/10.1016/j.cretres.2015.05.012.
Chipera, Steve J., and David L. Bish. 1995. 'Multireflection RIR and Intensity Normalizations for Quantitative Analyses: Applications to Feldspars and Zeolites.' *Powder Diffraction* 10 (1): 47–55. https://doi.org/10.1017/S0885715600014305.
———. 2002. 'FULLPAT: A Full-Pattern Quantitative Analysis Program for X-Ray Powder Diffraction Using Measured and Calculated Patterns'. *Journal of Applied Crystallography* 35: 744–49. https://doi.org/10.1107/S0021889802017405.
———. 2013. 'Fitting Full X-Ray Diffraction Patterns for Quantitative Analysis: A Method for Readily Quantifying Crystalline and Disordered Phases'. *Advances in Materials Physics and Chemistry* 3: 47–53. https://doi.org/10.4236/ampc.2013.31A007.
Chung, Frank H. 1974a. 'Quantitative Interpretation of X-Ray Diffraction Patterns of Mixtures. I1. Adiabatic Principle of X-Ray Diffraction Analysis of Mixtures'. *Journal of Applied Crystallography* 7: 526–31. https://doi.org/10.1107/s0021889874010387.
———. 1974b. 'Quantitative Interpretation of X-Ray Diffraction Patterns of Mixtures. I. Matrix-Flushing Method for Quantitative Multicomponent Analysis'. *Journal of Applied Crystallography* 7: 519–25. https://doi.org/10.1107/s0021889874010375.
Davis, Briant L., and Deane K. Smith. 1988. 'Tables of Experimental Reference Intensity Ratios'. *Powder Diffraction* 3 (4): 205–8. https://doi.org/10.1017/S088571560001349X.
Davis, Briant L., Deane K. Smith, and Mark A. Holomany. 1989. 'Tables of Experimental Reference Intensity Ratios Table No. 2, December, 1989'. *Powder Diffraction* 4 (4): 201–5. https://doi.org/10.1017/S0885715600013725.
Dere, Ashlee D., Timothy S. White, Richard H. April, Brian Reynolds, Thomas E. Miller, Elizabeth P. Knapp, Larry D. McKay, and Susan L. Brantley. 2013. 'Climate Dependence of Feldspar Weathering in Shale Soils

along a Latitudinal Gradient'. *Geochimica et Cosmochimica Acta* 122 (1): 101–26. https://doi.org/10.1016/j.gca.2013.08.001.
Dinis, Pedro, Eduardo Garzanti, Pieter Vermeesch, and João Huvi. 2017. 'Climatic Zonation and Weathering Control on Sediment Composition (Angola).' *Chemical Geology* 467: 110–21. https://doi.org/10.1016/j.chemgeo.2017.07.030.
Eberl, Dennis D. 2003. 'User's Guide to RockJock -- A Program for Determining Quantitative Mineralogy from Powder X-Ray Diffraction Data'. *U.S. Geological Survey* 2003 (78). https://doi.org/10.3133/ofr200378.
Egawa, Kosuke, Okio Nishimura, Shoko Izumi, Eiji Fukami, Yusuke Jin, Masato Kida, Yoshihiro Konno, et al. 2015. 'Bulk Sediment Mineralogy of Gas Hydrate Reservoir at the East Nankai Offshore Production Test Site.' *Marine and Petroleum Gology* 66: 379–87. http://dx.doi.org/10.1016/j.marpetgeo.2015.02.039.
Foster, Michael S., Gilberto M. Amado Filho, Nicholas A. Kamenos, Rafael Riosmena-Rodríguez, and Diana L. Steller. 2013. 'Rhodoliths and Rhodolith Beds'. *Smithsonian Contributions to the Marine Sciences* 39: 143–55. https://doi.org/doi:10.5479/si.1943667X.39.
Gavish, Eliezer, and Gerald M. Friedman. 1973. 'Quantitative Analysis of Calcite and Mg-Calcite by X-Ray Diffraction: Effect of Grinding on Peak Height and Peak Area'. *Sedimentology* 20: 437–44. https://doi.org/10.1111/j.1365-3091.1973.tb01621.x.
Hillier, Stephen. 1999. 'Use of an Air Brush to Spray Dry Samples for X-Ray Powder Diffraction'. *Clay Minerals* 34: 127–35. https://doi.org/10.1180/000985599545984.
———. 2000. 'Accurate Quantitative Analysis of Clay and Other Minerals in Sandstones by XRD: Comparison of a Rietveld and a Reference Intensity Ratio (RIR) Method and the Importance of Sample Preparation'. *Clay Minerals* 35: 291–302. https://doi.org/10.1180/000985500546666.
———. 2003. 'Quantitative Analysis of Clay and Other Minerals in Sandstones by X-Ray Powder Diffraction (XRPD)'. *International Association of Sedimentologists Special Publications* 34: 213–51. https://doi.org/10.1002/9781444304336.
Hjulström, F. 1939. 'Transportation of Detritus by Moving Water.' *Recent Marine Sediments, a Symposium* 5 (31).
Hubbard, Camden R., and Robert L. Snyder. 1988. 'RIR - Measurement and Use in Quantitative XRD'. *Powder Diffraction* 3 (2): 74–77. https://doi.org/10.1017/S0885715600013257.
Kuhlmann, Gesa, Poppe L. de Boer, Rolf B. Pedersen, and Theo E. Wong. 2004. 'Provenance of Pliocene Sediments and Paleoenvironmental Changes in the Southern North Sea Region Using Samarium–Neodymium (Sm/Nd) Provenance Ages and Clay Mineralogy.' *Sedimentary Geology* 171 (1–4): 205–26. https://doi.org/doi:10.1016/j.sedgeo.2004.05.016.
Liu, Zhifei, Shouting Tuo, Christophe Colin, James T. Liu, Chi-Yue Huang, Kandasamy Selvaraj, Chen-Tung Arthur Chen, et al. 2008. 'Detrital Fine-Grained Sediment Contribution from Taiwan to the Northern South China Sea and Its Relation to Regional Ocean Circulation.' *Marine Geology* 255 (3–4): 149–55. https://doi.org/10.1016/j.margeo.2008.08.003.
Marcano, Maria C., Tracy D. Frank, Samuel B. Mukasa, K. C. Lohmann, and Marco Taviani. 2015. 'Diagenetic Incorporation of Sr into Aragonitic

Bivalve Shells: Implications for Chronostratigraphic and Palaeoenvironmental Interpretations.' *The Depositional Record* 1 (1): 38–52. https://doi.org/10.1002/dep2.3.
Moore, Duane M., and Robert C. Reynolds. 1997. *X-Ray Diffraction and the Identification and Analysis of Clay Minerals*. 2nd ed. Oxford: Oxford University Press.
Nagtegaal, P. J. C. 1972. 'Depositional History and Clay Minerals of the Upper Cretaceous Basin in the South-Central Pyrenees, Spain.' *Leidse Geologische Mededelingen* 47 (2): 251–75.
Nagtegaal, P. J. C., A. Van Vliet, and J. Brouwer. 1983. 'Syntectonic Coastal Offlap and Concurrent Turbidite Deposition: The Upper Cretaceous Aren Sandstone in the South-Central Pyrenees, Spain.' *Sedimentary Geology* 34 (2–3): 185–218.
Nesbitt, H.W., C.M. Fedo, and G.M. Young. 1997. 'Quartz and Feldspar Stability, Steady and Non-Steady-State Weathering, and Petrogenesis of Siliciclastic Sands and Muds.' *The Journal of Geology* 105 (2): 173–92. https://doi.org/10.1086/515908.
Nesbitt, H.W., and G.M. Young. 1989. 'Formation and Diagenesis of Weathering Profiles.' *The Journal of Geology* 97 (2): 129–47. https://doi.org/10.1086/629290.
———. 1996. 'Petrogenesis of Sediments in the Absence of Chemical Weathering: Effects of Abrasion and Sorting on Bulk Composition and Mineralogy.' *Sedimentology* 43 (2): 341–58. https://doi.org/10.1046/j.1365-3091.1996.d01-12.x.
Ortiz, Joseph D., Leonid Polyak, Jacqueline M. Grebmeier, Dennis Darby, Dennis D. Eberl, Sathy Naidu, and Doron Nof. 2009. 'Provenance of Holocene Sediment on the Chukchi-Alaskan Margin Based on Combined Diffuse Spectral Reflectance and Quantitative X-Ray Diffraction Analysis'. *Global and Planetary Change* 68: 73–84. https://doi.org/10.1016/j.gloplacha.2009.03.020.
Pearson, M.J., and J.S. Small. 1988. 'Illite-Smectite Diagenesis and Palaeotemperatures in Northern North Sea Quaternary to Mesozoic Shale Sequences'. *Clay Minerals* 23: 109–32. https://doi.org/10.1180/claymin.1988.023.2.01.
Pecharsky, Vitalij K., and Peter Y. Zavalij. 2009. 'Collecting Quality Powder Diffraction Data'. In *Fundamentals of Powder Diffraction and Structural Characterization of Materials*, 2nd ed., 301–46. Boston, MA: Springer. https://doi.org/10.1007/978-0-387-09579-0 12.
Post, Jeffrey E., and David L. Bish. 1989. 'Rietveld Refinement of Crystal Structures Using Powder X-Ray Diffraction Data.' In *Modern Powder Diffraction*, 20:277–308. Reviews in Mineralogy & Geochemistry. Washington, D.C.: Mineralogical Society of America. https://doi.org/10.1515/9781501509018-012.
Raven, Mark D., and Peter G. Self. 2017. 'Outcomes of 12 Years of the Reynold's Cup Quantitative Mineral Analysis Round Robin'. *Clays and Clay Minerals* 65 (3): 122–34. https://doi.org/10.1346/CCMN.2017.064054.
Ridgwell, Andy, and Richard E. Zeebe. 2005. 'The Role of the Global Carbonate Cycle in the Regulation and Evolution of the Earth System.' *Earth and Planetary Science Letters* 234 (3–4): 299–315. https://doi.org/doi:10.1016/j.epsl.2005.03.006.
Robles-Salcedo, Raquel, Gonzalo Rivas, Vicent Vicedo, and Esmeralda Caus. 2013. 'Paleoenvironmental Distribution of Larger Foraminifera in

Upper Cretaceous Siliciclastic–Carbonate Deposits (Arén Sandstone Formation, South Pyrenees, Northeastern Spain).' *Palaios* 28 (9): 637–48. https://doi.org/10.2110/palo.2012.p12-125r.

Scheffler, Kay, Dieter Buehmann, and Lorenz Schwark. 2006. 'Analysis of Late Palaeozoic Glacial to Postglacial Sedimentary Successions in South Africa by Geochemical Proxies – Response to Climate Evolution and Sedimentary Environment'. *Palaeogeography, Palaeoclimatology, Palaeoecology* 240 (1–2): 184–203. https://doi.org/10.1016/j.palaeo.2006.03.059.

Schreiner, Walter N. 1995. 'A Standard Test Method for the Determination of RIR Values by X-Ray Diffraction.' *Powder Diffraction* 10 (1): 25–33. https://doi.org/10.1017/S0885715600014263.

Smith, Deane K., Gerald G. Johnson, and Alexandre Scheible. 1987. 'Quantitative X-Ray Powder Diffraction Method Using the Full Diffraction Pattern'. *Powder Diffraction* 2 (2): 73–77. https://doi.org/10.1017/S0885715600012409.

Środoń, Jan. 2006. 'Identification and Quantitative Analysis of Clay Minerals'. In *Handbook of Clay Science*, 1:765–87. Developments in Clay Science. Elsevier. https://doi.org/10.1016/S1572-4352(05)01028-7.

Środoń, Jan, Victor A. Drits, Douglas K. McCarty, Jean C.C. Hsieh, and Dennis D. Eberl. 2001. 'Quantitative X-Ray Diffraction Analysis of Clay-Bearing Rocks from Random Preparations'. *Clays and Clay Minerals* 49 (6): 514–28. https://doi.org/10.1346/CCMN.2001.0490604.

Środoń, Jan, M. Kotarba, A. Biroň, P. Such, N. Clauer, and A. Wójtowicz. 2006. 'Diagenetic History of the Podhale-Orava Basin and the Underlying Tatra Sedimentary Structural Units (Western Carpathians): Evidence from XRD and K-Ar of Illite-Smectite'. *Clay Minerals* 41: 751–74. https://doi.org/10.1180/0009855064130217.

Sundborg, Å. 1956. 'The River Klarälven a Study of Fluvial Processes'. *Geografiska Annaler* 38 (2–3): 125–316. https://doi.org/10.1080/20014422.1956.11880887.

Suttner, L.J., and P.K. Dutta. 1986. 'Alluvial Sandstone Composition and Paleoclimate; I, Framework Mineralogy.' *Journal of Sedimentary Research* 56 (3): 329–45. https://doi.org/10.1306/212F8909-2B24-11D7-8648000102C1865D.

Toby, Brian H. 2006. 'R Factors in Rietveld Analysis: How Good Is Good Enough?' *Powder Diffraction* 21 (1): 67–70. https://doi.org/DOI: 10.1154/1.2179804$.

Zhou, Xiang, Dong Liu, Hongling Bu, Liangliang Deng, Hongmei Liu, Peng Yuan, Peixin Du, and Hongzhe Song. 2018. 'XRD-Based Quantitative Analysis of Clay Minerals Using Reference Intensity Ratios, Mineral Intensity Factors, Rietveld, and Full Pattern Summation Methods: A Critical Review'. *Solid Earth Sciences* 3: 16–29. https://doi.org/10.1016/j.sesci.2017.12.002.

Appendices

8.1. Appendix 1

1.1. Average absolute biases in wt% per mineral for each RIR strategy.

McCrone mill homogenised				
Mineral	**Area – multipeak**	**Area – single peak**	**Height – multipeak**	**Height – single peak**
Quartz	36.92	27.80	3.74	1.69
Calcite	3.49	0.96	1.60	2.52
Ca-montmorillonite	22.73	24.34	9.48	2.28
Labradorite	0.63	1.88	1.46	4.00
Microcline	2.90	4.58	0.96	3.88
Average	**13.33**	**11.91**	**3.45**	**2.87**
Manually homogenised				
Quartz	44.96	37.32	5.77	5.61
Calcite	2.23	3.84	3.54	6.72
Ca-montmorillonite	27.07	27.03	13.16	12.57
Labradorite	1.32	3.40	4.09	6.91
Microcline	2.67	4.55	1.49	4.37
Average	**15.65**	**15.23**	**5.61**	**7.24**

8.2. Appendix 2

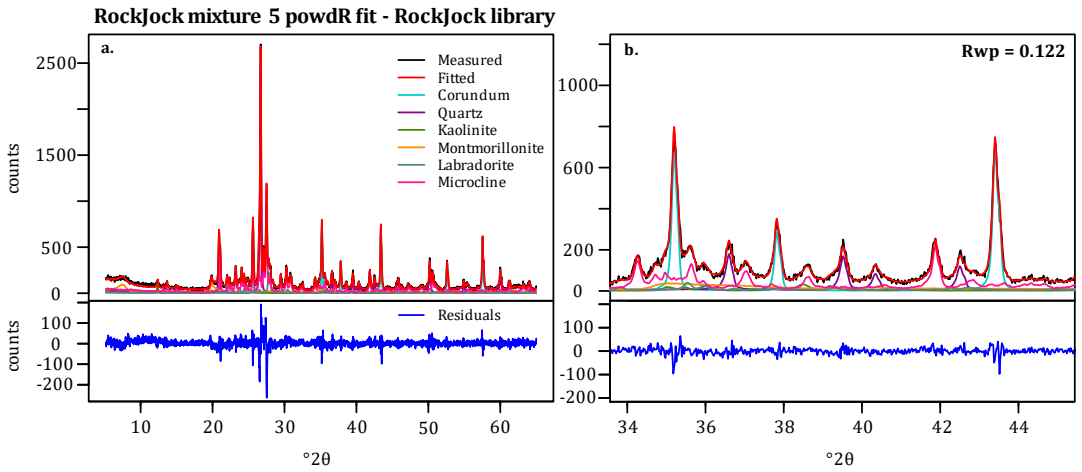

2.1. Manual full pattern summation powdR fit for RockJock mixture 5, analysed with the RockJock reference library. **a.** the entire fitted pattern (top) and the residuals (bottom). **b.** a section of the pattern (top) and the residuals (bottom), highlighting the fit. The fit is good, indicated visually as well as by the Rwp value (panel b, top right).

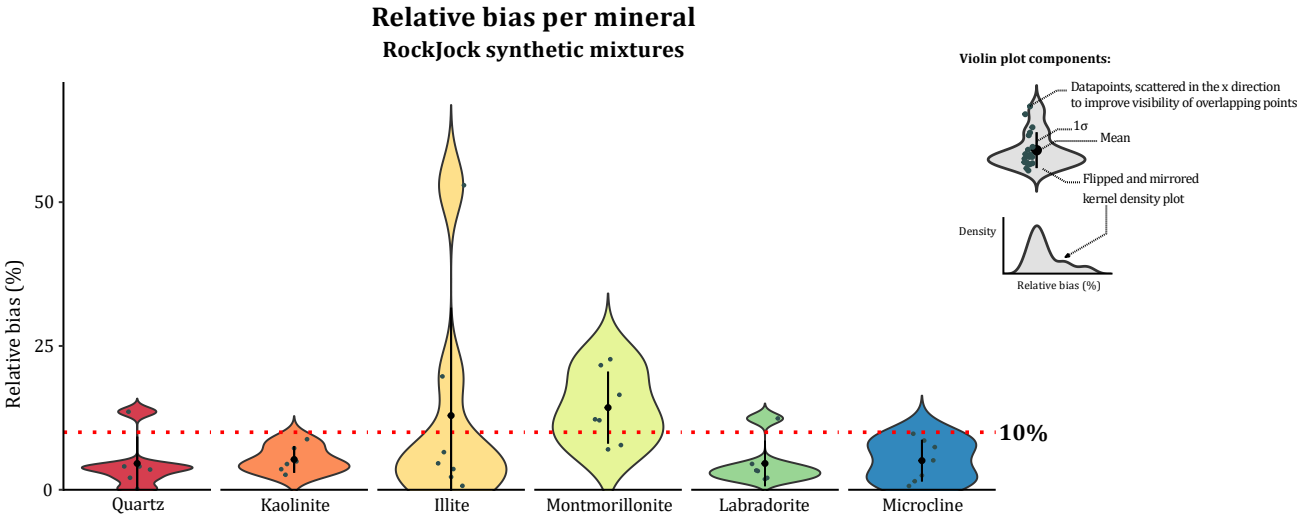

2.2. Violin plot showing the relative bias per mineral for the RockJock synthetic mixtures 1-8. Except for montmorillonite, the majority of the relative biases of each mineral falls below the 10% limit, indicating excellent accuracy.

2.3. PowdR results for RockJock mixture 5 quantified with the RockJock library. Settings: manual full pattern summation, 20 wt% corundum internal standard, no detection limit.

Mineral	Phase ID	RIR	Detected wt%	Actual wt%	Absolute bias [wt%]	Relative bias [%]
Corundum	CORUNDUM	1.00	20	20	0	0
Quartz	QUARTZ	3.54	19.97	20	0.03	0.15
Microcline	ORDERED_MICROCLINE	0.97	33.33	36	2.67	7.42
Labradorite	LABRADORITE	0.81	7.85	8	0.15	1.85
Kaolinite	KAOLINITE_DRY_BRANCH	0.58	4.29	4	0.29	7.22
Montmorillonite	MONTMORILLONITE_WYO	0.32	11.21	12	0.79	6.56
Total			**96.65**	**100**	**3.92**	

2.4. Average absolute biases in wt% per mineral for the RockJock mixtures 1-8, quantified with the RockJock library.

Quartz	Kaolinite	Illite	Montmorillonite	Labradorite	Microcline
0.47	0.66	1.01	2.61	0.89	0.71
Average: 1.06					

8.3. Appendix 3

3.1. PowdR results for RockJock mixture 5 quantified with this study's library. Settings: manual full pattern summation, 20 wt% corundum internal standard, no detection limit. Note that kaolinite is not present in this study's library, which accounts for some of the error.

Mineral	Phase ID	RIR	Detected wt%	Actual wt%	Absolute bias [wt%]	Relative bias [%]
Corundum	COR_AlfaAeasar_1	1.00	20	20	0	0

Quartz	Q_Merck_1	8.11	11.35	20	8.65	43.25
Microcline	MICRO_UU_1	2.07	12.25	36	23.75	65.96
Labradorite	LABRA_UU_1	2.41	4.92	8	3.08	38.54
Kaolinite	-	-	0	4	4	-
Ca-montmorillonite	CA.MO_SAz1_1	1.03	7.56	12	4.44	37.00
Total			**56.08**	**100**	**39.92**	

3.2. PowdR results for RockJock mixture 5 quantified with this study's library, but using RockJock RIRs. Settings: manual full pattern summation, 20 wt% corundum internal standard, no detection limit.

Mineral	**Phase ID**	**RIR**	**Detected wt%**	**Actual wt%**	**Absolute bias [wt%]**	**Relative bias [%]**
Corundum	COR_AlfaAeasar_1	1.00	20	20	0	0
Quartz	Q_Merck_1	3.54	25.99	20	5.99	29.94
Microcline	MICRO_UU_1	0.60	42.30	36	6.30	17.51
Labradorite	LABRA_UU_1	0.81	14.60	8	6.60	82.50
Kaolinite	-	-	0	4	4	-
Montmorillonite	CA.MO_SAz1_1	0.29	26.96	12	14.96	124.70
Total			**129.85**	**100**	**37.85**	

8.4. Appendix 4

4.1. RockJock mixture 5 quantified with the RockJock library. Settings: automatic full pattern summation, 20 wt% corundum internal standard, no detection limit. Bolded minerals are actually present in the mixture.

Mineral	Mineral ID	RIR	Detected wt%	Actual wt%	Absolute bias [wt%]
Corundum	**CORUNDUM**	**1.00**	**20.00**	**20**	**0.00**
Quartz	**QUARTZ**	**3.54**	**19.91**	**20**	**0.09**
Microcline	**ORDERED_MICROCLINE**	**0.97**	**31.59**	**36**	**4.41**
Labradorite	**LABRADORITE**	**0.81**	**4.11**	**8**	**3.89**
Kaolinite	**KAOLINITE_DRY_BRANCH**	**0.58**	**3.33**	**4**	**0.67**
Mont-morillonite	**MONTMORILLONITE_WYO**	**0.32**	**6.78**	**12**	**5.22**
Background	BACK_NEG	10000.00	0.00	0	0.00
Orthoclase	ORTHOCLASE	0.58	0.73	0	0.73
Oligoclase	OLIGOCLASE_NORWAY	0.76	0.45	0	0.45
Andesine	ANDESINE	0.82	2.13	0	2.13
Anorthite	ANORTHITE	0.53	1.20	0	1.20
Dolomite	FE_DOLOMITE	1.76	0.10	0	0.10
Siderite	SIDERITE	2.06	0.18	0	0.18
Halloysite	HALLOYSITE	0.24	0.79	0	0.79
Mont-morillonite	CA_MONTMORILLONITE	0.29	0.38	0	0.38
Illite	ILLITE_1MD	0.24	1.83	0	1.83
Mica	BIOTITE_1M	0.69	0.39	0	0.39
Serpentine	BERTHIERINE	0.37	0.60	0	0.60

Amphibole	AMPHIBOLE	0.53	0.09	0	0.09
Anhydrite	ANHYDRITE	1.57	0.10	0	0.10
Magnetite	MAGNETITE	1.91	0.45	0	0.45
Garnet	ALMANDINE_GARNET	1.89	0.15	0	0.15
Ilmenite	ILMENITE	0.98	0.01	0	0.01
Charcoal	CHARCOAL	0.06	2.29	0	2.29
Analcime	ANALCIME	1.67	0.01	0	0.01
Galena	GALENA	7.97	0.00	0	0.00
Zircon	ZIRCON	4.16	0.10	0	0.10
Sulphur	SULFUR	1.93	0.16	0	0.16
Tridymite	TRIDYMITE_POOR	0.11	5.22	0	5.22
Psilomelane	PSILOMELANE	0.37	0.34	0	0.34
Smectite	SMECTITE_AND_AMORPH_BETTASO	0.22	1.21	0	1.21
Diaspore	DIASPORE	1.17	0.03	0	0.03
Pyroxene	ENSTATITE	0.26	0.14	0	0.14
Cordierite	CORDIERITE	0.73	0.37	0	0.37
Nahcolite	NAHCOLITE	0.78	0.09	0	0.09
Total			**105.25**	**100**	**33.81**

8.5. Appendix 5

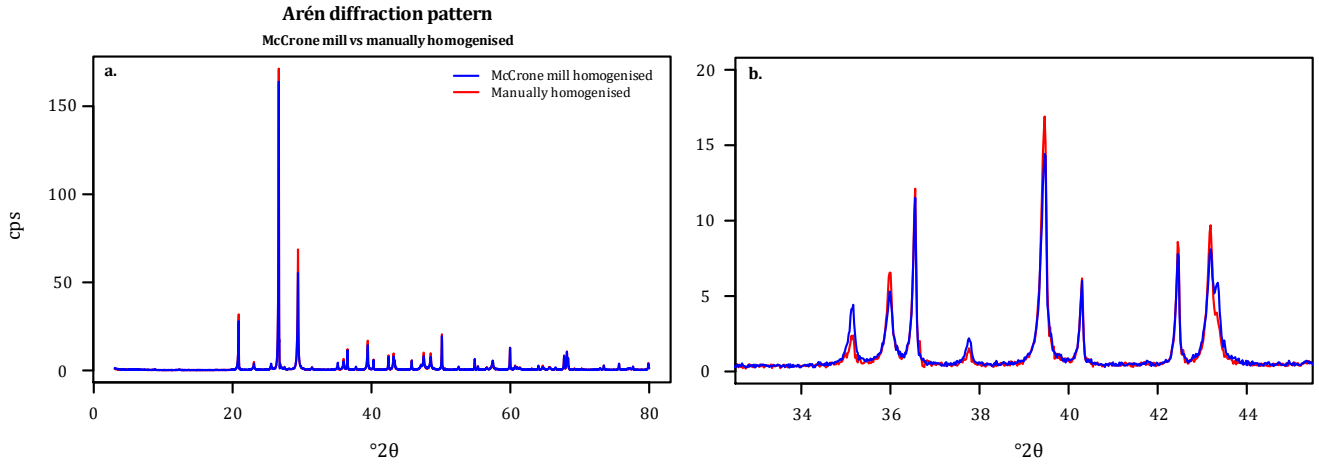

5.1. Manually vs McCrone mill homogenised Arén XRD patterns. **a.** the entire pattern. **b.** a section of this pattern. Most peaks are higher for the manually homogenised sample, as in the synthetic rock mixtures. There appears to be no consistent offset along the °2θ axis between the two patterns.